Homoplasmic deleterious MT-ATP6/8 mutations in adult patients

Benoit Rucheton, Claude Jardel, Sandrine Filaut, Maria del Mar Amador, Thierry Maisonobe, Isabelle Serre, Norma Beatriz Romero, Sarah Leonard-Louis, Francis Haraux, Anne Lombès

Homoplasmic deleterious *MT-ATP6/8* mutations in adult patients

Benoit Rucheton*[a], Claude Jardel[a], Sandrine Filaut[a], Maria del Mar Amador[b], Thierry Maisonobe[c], Isabelle Serre[d], Norma Beatriz Romero[e], Sarah Leonard-Louis[c], Francis Haraux[f], Anne Lombès*[g]

[a] Service de Biochimie Métabolique, Centre de génétique moléculaire et chromosomique, CHU Pitié-Salpêtrière, AP-HP, Paris, France

[b] Département de Neurologie, CHU Pitié-Salpêtrière, AP-HP, Paris, France

[c] Département de Neurophysiologie Clinique et de Neuropathologie, CHU Pitié-Salpêtrière, AP-HP, Paris, France ; Sorbonne Université, UPMC Univ Paris 06

[d] Département de Neurologie, CHU Reims, Reims, France

[e] Center for Research in Myology, CHU Pitié-Salpêtrière; Sorbonne Université, UPMC Univ Paris 06; INSERM UMRS974, Paris, France.

[f] Institute for Integrative Biology of the Cell (I2BC), CEA, CNRS, Université Paris-Sud, Université Paris-Saclay, Gif-sur-Yvette, France

[g] INSERM U1016 Institut Cochin; CNRS UMR 8104; Université Paris-Decartes-Paris5, Paris, France

*Corresponding author: Dr Anne Lombès, Faculté de médecine Cochin, INSERM U1016, 24, rue du Faubourg St Jacques, 75014 Paris, France, phone (33) 1 53732753; FAX (33) 1 53732757; mail: anne.lombes@inserm.fr and Benoit Rucheton, Service de Biochimie Métabolique, Centre de génétique moléculaire et chromosomique, CHU Pitié-Salpêtrière, 81, bd de l'Hôpital 75013 Paris, France, phone (33) 1 42177655, mail benoit.rucheton@aphp.fr

Highlights

1. Numerous homoplasmic *MT-ATP6/8* missense mutations are potentially deleterious (putative) mutations
2. Functional analyses disclose striking gradation in severity and tissue-specific expression
3. Efficient compensation of deleterious *MT-ATP6/8* mutations appears common
4. Under-diagnosis of human complex V defect is a likely hypothesis
5. With respect to diagnosis, fibroblasts are most often non informative

Abstract

To address the frequency of complex V defects, we systematically sequenced *MT-ATP6/8* genes in 512 consecutive patients.

We performed functional analysis in muscle or fibroblasts for 12 out of 27 putative homoplasmic mutations and in cybrids for four. Fibroblasts, muscle and cybrids with known deleterious mutations underwent parallel analysis. It included oxidative phosphorylation spectrophotometric assays, western blots, structural analysis, ATP production, glycolysis and cell proliferation evaluation.

We demonstrated the deleterious nature of three original mutations. Striking gradation in severity of the mutations consequences and differences between muscle, fibroblasts and cybrids implied a likely under-diagnosis of human complex V defects.

Keywords

Mitochondrial DNA; ATP synthase; cybrids; oxidative phosphorylation; mitochondrial disease; homoplasmy.

Graphical abstract

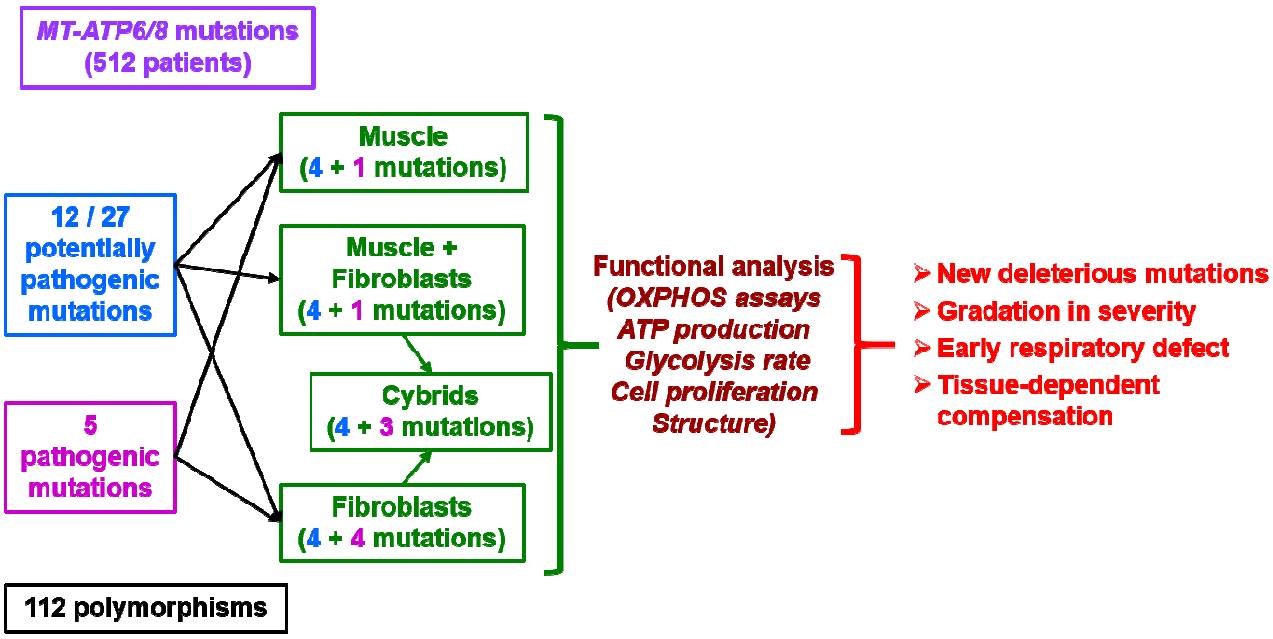

1. Introduction

1.1 $F_o F_1$ ATP synthase

$F_o F_1$ ATP synthase (EC 7.1.2.2), complex V of the mitochondrial oxidative phosphorylation pathway (OXPHOS), produces the vast majority of ATP in humans. Its 17 structural subunits compose two domains (Fo, associated with the inner mitochondrial membrane, and F_1, located in the mitochondrial matrix), connected by two stalks that couple the proton transfer in F_o with ATP synthesis or lysis in F_1. Two mitochondrial DNA (mtDNA) genes (*MT-ATP6* and *MT-ATP8*) encode two structural subunits of complex V (subunit a and A6L respectively), both located in the F_o domain, while nuclear genes encode all the other structural subunits as well as all complex V assembly factors.

1.2 Human diseases due to defective Fo F_1 ATP synthase

Among human mitochondrial diseases, defined as the diseases due to defective OXPHOS, ATP synthase defects appeared as very rare (Gorman et al., 2015, Gorman et al., 2016). The first identified genetic alteration causing human ATP synthase defect was a point mutation in the mtDNA *MT-ATP6* gene (m.8993T>G) changing a highly conserved leucine into arginine (Holt et al., 1990). Since then, mutations of other genes causing defective ATP synthase further demonstrated the reality of that defect in human pathology (Hejzlarova et al., 2014, Dautant et al., 2018). Mutations of seven nuclear genes have been associated to disease (*ATP5F1E*, *ATP5F1A*, *ATP5F1D, ATP12*, *TMEM70*, *USMG5,* and *OXA1L)* (De Meirleir et al., 2004, Cizkova et al., 2008, Mayr et al., 2010, Jonckheere et al., 2013, Barca et al., 2018, Olahova et al., 2018, Thompson et al., 2018)). These nuclear DNA alterations affected few patients. While few dozen patients presented with *TMEM70* mutations (Hejzlarova et al., 2014), only one to three patients had mutations of each other gene. Demonstration of the deleterious nature of these nuclear genes mutations has been straightforward. It relied on functional complementation of the enzymatic defect in patients' cells (Cizkova et al., 2008, Jonckheere et al., 2013, Barca et al., 2018) and/or reproduction of the defect

by genetic engineering of yeast, drosophila or immortal cell lines (Havlickova et al., 2010, Meulemans et al., 2010, Olahova et al., 2018).

In contrast, despite their small size (681 and 207 base pairs for *MT-ATP6* and *MT-ATP8* respectively), the two mtDNA located genes showed 46 different mutations associated to disease (see Mitomap at https://www.mitomap.org) (Kogelnik et al., 1997, Dautant et al., 2018). However, direct demonstration of their deleterious nature most often lacked, in great part because of the difficult engineering of mtDNA. Recurrence in independent families in association with a similar phenotype has been a major criterion for considering a mtDNA mutation as "confirmed" (Kogelnik et al., 1997). It occurred for 11 mutations. In addition, 13 mutations, including six of the recurrent ones, have been transferred into cybrids, i.e. cytoplasmic hybrid cells with nuclear DNA from parental immortal cell line and mtDNA from patients (Trounce et al., 1994, Manfredi et al., 1999), or into yeast *Saccharomyces cerevisiae* (Rak et al., 2007) (Table e-1). Co-transfer of the mutation with significant decrease of mitochondrial ATP production directly demonstrated the mutation deleterious potential. For most mutations however, essentially indirect criteria suggested their deleterious nature. These criteria included absence of the mutation in controls, phylogenetic conservation of the mutated amino acid and, in the case of heteroplasmic mutations i.e. mutations coexisting with residual wild type mtDNA molecules, correlation among family members between the mutation proportion in blood and the severity of the clinical phenotype (Holt et al., 1990).

The clinical phenotypes associated with the mutations of either *MT-ATP6* or *MT-ATP8* (*MT-ATP6/8*) have been quite diverse, even when only considering the "confirmed" mutations or those demonstrated as co-segregating with an ATP synthase defect (Table e-1). Age at disease onset varied from neonatal period to adulthood; the earlier the onset, the more severe the outcome with premature death. In addition to variable severity, the targeted organs differed between patients. Myocardium, cerebellum, cerebral basal ganglia and motor neurons were the most frequently affected tissues but none of them was constantly involved. Some families presented with unexpected signs in mitochondrial diseases such as recurrent accesses of paralysis.

Families with an adult onset, relatively mild, phenotype and homoplasmic mutations (Pfeffer et al., 2012, Pitceathly et al., 2012, Synofzik et al., 2012, Auré et al., 2013) contradicted the link between mutation proportion and severity, initially proposed in families with patients with early onset severe encephalopathy (Gorman et al., 2016). This was true for several mutations changing a wild type leucine into proline. It never occurred with mutations at the same nucleotide position changing the wild type leucine into arginine. These "severe" mutations have constantly been only associated with severe, early onset, phenotypes (Holt et al., 1990, Carrozzo et al., 2001).

1.3 Addressing the incidence of MT-ATP6/8 deleterious mutations

Whatever their clinical presentation, patients with complex V defect did not present with any characteristic histological markers of mitochondrial myopathy. Their biochemical investigation rarely assessed muscle ATP synthase, most probably because routine diagnostic OXPHOS assays often does not include ATP synthase assay (Haraux and Lombes, 2019). As a result, the evaluation of the ATP synthase activity relied on fibroblasts, using different methods such as spectrophotometric assay of complex V-linked ATP hydrolysis, measurement of ATP production rate and/or respiratory control ratio. In some cases, different methods gave different results (Vazquez-Memije et al., 2009, Kucharczyk et al., 2010).

Based on the diversity of the clinical spectrum associated with ATP synthase defects, together with the lack of characteristic histological anomalies and the difficulties of biochemical investigations, we considered likely an under-diagnosis of these defects. Therefore, we addressed the frequency of mtDNA-related ATP synthase defects by systematically sequencing *MT-ATP6/8* genes in patients sent to La Salpêtrière hospital center for a suspected mitochondrial disease. That approach confirmed the high variability of these two genes and the frequency of missense mutations. After incidence and software analyses, 27 mutations remained putative, requiring functional analysis. We obtained a muscle fragment and/or cultured skin fibroblasts for 12 of these mutations. Depending on the available tissue, we evaluated complex V-linked ATP hydrolysis, rate of ATP production, OXPHOS activities and reliance of cell proliferation on oxidative energetics. We compared the

results with controls but also with samples with confirmed *MT-ATP6* deleterious mutations. To avoid biases due to cellular senescence of primary fibroblasts, we reiterated their analyses after transfection with the human telomerase catalytic subunit. For four mutations, we then obtained cybrids with homoplasmic mutation and assessed their functionality in comparison with cybrids with wild type mtDNA or homoplasmic confirmed mutations.

With these approaches, we could demonstrate the deleterious potential of three homoplasmic *MT-ATP6/8* mutations associated with late onset disease in adults. We also showed the complexity of the pathophysiological mechanisms of *MT-ATP6/8* mutations in cultured cells, including graded consequences and early respiratory chain involvement. With respect to diagnosis, fibroblasts appeared much less sensitive than muscle, strongly motivating the implementation of ATP synthase assay of muscle in routine diagnosis in order to improve identification of complex V defects.

2. Methods

2-1-Samples

This study was following the Declaration of Helsinki. Informed consent was obtained from the participants prior to their participation in the study, under protocols approved by the our Institutional Review Board.

An open muscle biopsy obtained the fragments for biochemical investigations that were immediately frozen and stored at -80°C until use. Cultured primary fibroblasts were derived from a forearm skin biopsy using standard procedure. All primary fibroblasts were before passage 18 when assayed. They were transduced with a retrovirus encoding the catalytic subunit of human telomerase as described (Auré et al., 2007). Control fibroblasts were from the tissue repository of the AFM (Association Française contre les Myopathies). Cytoplasmic hybrids (cybrids) were obtained from 143B rho0 cells and fibroblasts as described (King and Attardi, 1989).

2-2-DNA extraction

Extraction of DNA from muscle and cell pellets used standard methods based on proteinase K and SDS digestion, phenol/chloroform extraction and isopropanol precipitation. It used QIAamp DNA Mini Kit extraction (Qiagen, Courtaboeuf, France) for blood cells.

2-3-MT-ATP6/8 sequencing

We sequenced *MT-ATP6/8* on muscle DNA for all patients with a muscle biopsy and on blood DNA for the other patients. For the first 106 patients, we sequenced only *MT-ATP6/8* genes using Sanger method. For the following 406 patients, we obtained the sequence of *MT-ATP6/8* genes as part of the whole mtDNA sequence obtained using Sanger sequencing (analysis of all coding and non-coding regions) (213 patients), then the Nextera® XT DNA kit (Illumina, Eindhoven, The Netherlands), following the manufacturer protocol (193 patients). Sequence analysis used the software MiSeqReporter, MTDNA Variant Analyzer and Genodiag pipeline (Genodiag society, Paris France) with the updated consensus Cambridge sequence (GenBank accession number: NC_012920) as reference (Andrews et al., 1999)

We estimated the pathogenicity using Alamut Visual software (Interactive Biosoftware, France). This application provides the conservation of nucleotide, amino acid and assesses the physicochemical gap created between the wild type and mutant aminoacid thanks to different *in silico* prediction software (Align GVGD, Polyphen, Mutation taster and SIFT), which base their prediction on the variant frequency in the general population and conservation of the modified amino acid.

For all cultured cells, either fibroblasts or cybrids, we verified the presence and homoplasmic status of each mutation using appropriate restriction enzymes. For mutations m.8993T>C and m.8993T>G that cannot be differentiated by restriction analysis, which cuts the two mutant sequences, we added an allele-specific quantitative PCR allowing distinguishing the two mutations. Figure e-1 gives the sequences of the primers, the restriction enzyme and the method of the allele-specific PCR.

2-4-Spectrophotometric assays

For complex V-linked ATP hydrolysis assay in muscle, we used the protocol recently published (Haraux and Lombes, 2019). That protocol was set up for tissue samples but was not optimal for frozen cell pellets. We therefore modified the cell pellets preparation adding dilution at ~0.1 mg/mL protein in water and sonicating them twice during 5 seconds (Chretien et al., 1990). We also removed dodecylmaltoside from the assay mixture. These two modifications allowed obtaining reproducible values with satisfactory oligomycin sensitivity at 70±10, 64±7 and 69±11% in control primary fibroblasts, fibroblasts transduced with telomerase catalytic subunit and cybrids respectively.

All other spectrophotometric assays were as described in (Medja et al., 2009). For cell pellets, complex I assay used the sample preparation set up for complex V while all other assays used cell pellets suspended at 1 mg/mL in 225 mM mannitol, 75 mM sucrose, 0.1 mM EDTA and 10 mM Tris–HCl, pH 7.4 (Medja et al., 2009).

2-5-Cell analyses

Unless otherwise stated, culture medium was DMEM containing 5 mM glucose, 1 mM pyruvate, 10% fetal bovine serum and 50 IU/mL penicillin 50 µg/mL streptomycin.

2-5-1-Rate of ATP production

400000 cells collected using trypsin-EDTA and washed once with phosphate buffer saline were suspended in 200 µL respiration medium (5 mM K phosphate, 1 mM EGTA, 3 mM EDTA 100 mM K MES, pH 7.5) and permeabilized with 2 µL 0.4% digitonin (*i.e*. 20 µg digitonin per million cells) during 5 minutes. After taking samples for protein determination, bovine serum albumin was added to 0.8% final concentration and 50 µL of the cell suspension were incubated, in duplicates, in 50 µL of respiration medium with 20 mM pyruvate, 20 mM glutamate, 10 mM malate, 40 mM succinate, 2 mM ADP and 50 µM AP_5A, an adenylate kinase inhibitor. Incubation at 37°C, performed with constant stirring, started immediately. 10 µL samples were taken after 4 and 8 minutes. Two additional 10 µL samples were taken 4 and 8 minutes after addition of 20 µg/mL oligomycin. ATP bioluminescence assay kit HS II (Sigma-Aldrich) measured ATP concentration according to the

manufacturer instructions. Subtraction of the difference of ATP concentration between 4 and 8 minutes obtained after oligomycin addition from that between 4 and 8 minutes in the first incubation phase gave the ATP production rate expressed as nanomoles ATP produced per minute and milligram protein.

2-5-2-Cell proliferation assay

To analyze cell proliferation in galactose *versus* glucose, 3000 cells per well were seeded in six wells of four 24-well plates. After 24 hours, the culture medium was changed for DMEM without glucose, containing 1 mM pyruvate, 10% fetal bovine serum, antibiotics, completed with 5 mM galactose for half the wells or with 5 mM glucose for the other half. Cell numbering was performed in one plate every 24 hours (T0, T24, T48 and T72 plates) using the neutral red method (Repetto et al., 2008) and expressed as fold increase relative to T0. When cells did not grow at all or even died in the galactose medium, we compared proliferation in 5 mM glucose *versus* 22.5 mM glucose, instead of 5 mM galactose *versus* 5 mM glucose.

2-5-3-Lactate production

~100000 cells per well were seeded in 48-well plates. After 24 hours, the culture medium was replaced by 400 µL DMEM containing 5 mM glucose, 10% fetal bovine serum, and antibiotics. After two hours incubation at 37°C, 10 µL of the culture medium were taken for lactate measurement in 250 µM NAD, 50 µg/mL L-lactate dehydrogenase from rabbit muscle (Sigma), 200 mM hydrazine, 12 mM EDTA, 100 mM Tris HCl, pH 9.0. After four hours incubation at 37°C, reading at 340 nm measured the amount of NADH produced. Serial two-fold dilutions of lactate solution (Sigma, France) (from 2500 to 78 µM) and culture medium without cells incubated in parallel served as standards and background respectively. Results were expressed as nanomoles lactate produced in two hours per well. We then numbered cells in each well of the 48-well plates by measuring the DNA content of each well. After one wash with phosphate buffer saline, wells were filled with 200 µL 0.01% SDS and the 48-well plate was kept overnight at -20°C. After thawing, addition of 200 µL 1 M NaCl, 1 mM EDTA, 10 mM Tris, pH 7.4, 4 µg/mL bisbenzimide

Hoechst 33342 (Sigma, France) was followed by a two-hour incubation at room temperature with protection from light. Fluorescence signals (excitation/emission wavelength 355/465 nm) measured the DNA content in each well. Parallel treatment of serial dilutions of lambda DNA HindIII digest (from 2000 to 10 ng per well) provided standards. Results were expressed as number of cells per well, considering 10 picograms as the mass of the human diploid genome. They allowed normalization of the lactate production to the number of cells in the wells and its expression as nanomoles lactate produced in two hours per 10^3 cells.

2-6-Western blot procedure

Muscle supernatants, whole cell pellets or mitochondrial fractions were separated by SDS-PAGE on a linear 4 to 20% gradient polyacrylamide gel (Biorad) then transferred onto Immobilon-P membrane (Merck). Antibodies against ND1 and CO2 were produced in our group (Barthélémy et al., 2001), the other antibodies were from Abcam, either monoclonal anti-SDHA, anti-LMNA, anti-TOMM22 and anti-TUBA, polyclonal anti-ATP5B, anti-MT-ATP6. Primary antibodies were visualized using peroxidase-conjugated secondary antibodies (Sigma-Aldrich, France) and Pierce™ ECL Western Blotting Substrate (Life Technologies, USA). Quantification of the luminescent signals used volumes obtained after basal adjustment with rolling ball approach by Fusion FX (Vilber Company, Germany). Results were normalized to SDHA for the mitochondrial compartment and to TUBA for the muscle supernatants or LMNA for cell pellets and expressed as % of the mean signal from control samples analysed on the same membrane.

2-7-Structural analysis of Complex V

To locate the different mutated residues in Complex V, we visualized its tri-dimensional structure using Swiss-PdbViewer software. Since the full structure of human ATP synthase was not available, we used the published bovine model (Pdb entry *5fij*) for analyzing mutations of subunits 6, for which exists a definition at very high resolution. Since subunit 8 was not resolved in the bovine model, we used the published porcine model (Pdb entry *6j5i*) for analyzing subunit 8 mutations. In all the domains analyzed, the sequence homology between *H. sapiens*, *B. taurus* and

S. scrofa was very high. We verified that conclusions drawn from analysis of the bovine subunit 6 remained valid using the porcine one.

3. Results

3.1 MT-ATP6/8 genes present with numerous private variants

In 2011, following the identification of patients with episodic paralysis accesses due to homoplasmic *MT-ATP6/8* mutations (Auré et al., 2013), we added systematic sequencing of these two genes in the diagnostic flowchart applied in La Salpêtrière hospital to patients with suspected mitochondrial disease. As a whole, 874 variants were present in 512 patients, a minority of which (185 variants, 21%) were synonymous mutations while the remaining 689 variants induced 92 different missense mutations (Figure 1 and Table e-2). Among these, three mutations accounted for 62% of the observed variants because they reflected the presence of rare variants in the reference sequence (430 patients presented with the m.8860A>G p.Thr112Ala variant, 76 with the m.8701A>G p.Thr59Ala, and 40 with the m.9055G>A p.Ala177Thr). Five mutations were confirmed pathogenic mutations (m.8993T>C, m.8993T>G, m.9035T>C, m.9176T>C, and m.9185T>C). They occurred in 15 patients (2.9%) who presented with diverse clinical phenotypes from very severe, early onset, Leigh syndrome to pauci-symptomatic patients with episodic accesses of paralysis and late onset, slowly progressive, axonal peripheral neuropathy (Table 1). The remaining 84 missense mutations spanned the length of subunit a and AL (Figure e-2A). Each patient had from 1 to 10 variants with a mean of two variants per patient (Figure e-2B).

Most mutations occurred in only one patient giving an observed frequency of 0.2% (Figure e-2C). Our patients' population thus showed a predominance of private mutations similar to that observed in GenBank database. Therefore, ascribing pathogenicity could not use the rarity of the variant but, conversely, recurrent variants were probable neutral variants. Setting the frequency threshold for likely neutral variants was an arbitrary decision. We had to take into account the need to reduce the number of putative mutations while keeping in mind that a significant number of GenBank

sequences originate from patients. The threshold excluding variants reported more than 15 times in GenBank database led to exclude 64% of the mutations. It thus appeared reasonably conservative. We then analyzed the potential impact of the remaining 30 mutations combining several prediction software (Polyphen, GVGD, SIFT, evaluation of the Grantham distance and phylogenetic conservation of the modified aminoacid) and giving one point each time prediction was in favor of a deleterious mutation (Table e-3). Prediction software unanimously considered three mutations as nonpathogenic (m.8666A>G, m.8908T>C and m.8974C>T). We did not undertake any further study of these three mutations. Prediction software unanimously considered seven mutations (23%) as deleterious with a score of 6, identical to the score obtained with confirmed deleterious mutations. The 20 remaining mutations showed discrepancy between prediction methods with a majority (14 mutations) with at least half the prediction software proposing a deleterious impact.

3.2 Functional evaluation of the MT-ATP6/8 mutations

The possibility to address the functional relevance of the observed mutations depended on the availability of samples from the patients. We obtained a residual muscle fragment and/or cultured skin fibroblasts from 12 patients, including five of the patients with a mutation unanimously considered pathogenic by the prediction software (Table e-3). The absence of available sample prevented any further analysis for the two remaining mutations predicted as pathogenic (m.8639T>C and m.8999T>C). We obtained the complete mtDNA sequence and mtDNA haplotype for 11 patients of the 12 with available tissue samples (Table e-4).

3.2.1 Muscle analysis

The first step of analysis was the spectrophotometric evaluation of ATP synthase activity in muscle using its reverse reaction, i.e. ATP hydrolysis (Haraux and Lombes, 2019). In parallel to the muscles with putative mutations, we analyzed two muscle fragments from patients with confirmed mutations (Table 2). ATP synthase activity was below the tenth centile of control values in six muscles, including the two muscles with confirmed deleterious mutations. This was true when

considering the oligomycin sensitive activity or the activity sensitive to the addition of both oligomycin and IF1.

In five out of these six muscles, complex I activity was also below the tenth centile of control values. Rotenone sensitive complex I activity is the OXPHOS activity most sensitive to cryopreservation conditions (Sammut et al., 1998). In most samples, the proportion of the rotenone sensitive, specific, complex I activity in the total NADH oxidase activity was high (70±14%), tending to rule out an inappropriate sample preservation causing the observed defects. Furthermore, three complex I defects out of four were already present in the initial biochemical investigations performed prior to the mutation identification (Table 2). Western blot analysis of muscle proteins showed normal steady state level of ATPF1B, subunit of the complex V F_1 domain, in all the muscles whatever their complex V activity (Figure e-3) while MT-ATP6 subunit appeared decreased in the muscles with mutation m.9035T>C or m.8424T>C, reaching significance only for the latter. The mtDNA-encoded ND1subunit of complex I was decreased in the muscle with m.8975T>C mutation when normalized to the respiratory complex II SDHA subunit but increased when normalized to α tubulin, a microtubule component. Mitochondrial proliferation most probably explained that discrepancy. It was prominent in several muscles that disclosed several fold increase of the ratio of several mitochondrial proteins to α tubulin. Spearman correlation analyses showed that complex V activity tightly correlated with MT-ATP6 but not ATPF1B steady state thus confirming that the ATP hydrolysis assay measured fully assembled complex V activity and not that of isolated F_1 domains (Haraux and Lombes, 2019).

The small size of the residual muscle fragments did not allow for further in depth analysis of the observed OXPHOS alterations. We therefore sought to obtain an alternative, non-invasive, tissue.

3.2.2 Analysis of primary skin fibroblasts

Cultured skin fibroblasts offer the possibility to address complex V function by different approaches and in repeated assays. However, the results of these assays have sometimes given contradictory results (Vazquez-Memije et al., 2009, Kucharczyk et al., 2010). To avoid bias due to

specific cell lines, we used 10 different cell lines derived from control subjects to build up the control group. In addition, taking opportunity of the recurrence of confirmed deleterious mutations, we derived several fibroblasts lines with the same mutation. Three lines had the m.8993T>G mutation, constantly associated with a severe disease, occurring in infants and leading to early death. Eight lines had mutations associated with less severe phenotypes occurring in adults (m.9185T>C in four lines, m.8993T>C in three lines and m.9035T>C in one line). Using PCR-based methods, we checked the presence and homoplasmy of all these mutations in the initial cell cultures and thereafter along the study (Figure e-1).

All fibroblasts with a confirmed deleterious mutation and those with the m.8424T>C mutation disclosed significant decrease of their rate of ATP production by OXPHOS (Figure 2A). However, none of these lines had any significant defect of the complex V activity as measured by ATP hydrolysis assay (Figure 2B). In contrast, six lines, five with potential mutations and one with the confirmed m.8993T>G mutation, presented with significant complex I and/or complex IV defect (Figure 2C to 2F).

To assess the functional relevance of the observed defects, we compared the cell proliferation in culture medium containing either 5 mM glucose or 5 mM galactose, the latter condition increasing the cells reliance on OXPHOS (Figure 2G). All cells with confirmed mutations tended to have a high ratio of doubling time in galactose *versus* glucose, reaching significance for three mutations out of four. Three cells lines with putative mutations showed significant increase of that same ratio, two of them (m.8424T>C and m.8975T>C) almost stopping their proliferation in galactose.

To address the relative relevance of the diverse parameters, we analyzed their relationship in seven different control fibroblast lines using Spearman correlation test (Figure 2H). ATP production rate showed the expected negative correlation with the ratio of doubling time in galactose *versus* glucose ($p=0.005$) and the expected positive relationship with complex I activity, complex I being the major entry of electrons into the respiratory chain ($p=0.029$). However, the expected negative relationship between complex I activity and the ratio of doubling time in galactose *versus* glucose failed to reach

significance (p=0.103). None of the other spectrophotometrically measured OXPHOS activities disclosed any significant correlation with ATP production rate or ratio of doubling time in galactose *versus* glucose.

3.2.3 Analysis of skin fibroblasts transduced with the human telomerase catalytic subunit

Relative senescence of the primary fibroblasts is a well-known factor altering cellular proliferation, tricarboxylic acid cycle and oxidative phosphorylation (Hernandez-Segura et al., 2018). It might prematurely occur in cells with OXPHOS defect. Therefore, to exclude senescence causing the variability of the anomalies observed in complex V mutant cells, we transduced mutant and control cell lines with the telomerase catalytic subunit together with puromycin resistance. Transduction failed for one mutant cell line with the m.9008C>G mutation. After one-month puromycin selection, we verified the presence of the mutation using restriction PCR (Figure e-1). We then performed OXPHOS analyses in cells grown in normal culture medium without puromycin for at least one passage.

As previously observed (Auré et al., 2007), the rate of ATP production of both control and mutant fibroblasts transduced by telomerase tightly correlated with that of their primary counterpart, albeit at a lower level (Figure 3A). For the fibroblasts with confirmed deleterious mutations, telomerase transduction erased the significance of the decreased ATP production for mutations m.8993T>C, m.9035T>C and m.9185T>C but not for the severe m.8993T>G mutation (Figure 3B). Among the cells with putative mutations, the defect of ATP production remained significant for the m.8424T>C mutation and became significant for those with the m.8975T>C mutation.

With respect to the OXPHOS spectrophotometric assays, the sole spectrophotometric defect significant in both primary and transduced fibroblasts was the defective complex I observed in cells with the m.8424T>C mutation (Figure 3C to 3G).

Telomerase transduction did not modify the cells doubling times (2.1 days in 5 mM glucose and 2.6 in galactose in control primary fibroblasts *versus* 2.4 and 3.0 in control fibroblasts transduced by telomerase, p=0.2 and 0.16 respectively). It did not erase any significantly increased ratio of

doubling time in galactose *versus* glucose previously observed in primary fibroblasts but it prevented the almost complete growth arrest previously observed in the primary fibroblasts with either m.8424T>C or m.8975T>C mutation, showing the impact of senescence (Figure 3H).

3.2.4 Analysis of 143B cybrid cells

Using the analyses of fibroblasts, both primary and transduced with telomerase, we undertook the transfer into 143B rho0 cells of the m.8424T>C and m.8975T>C mutation that were associated with significant defect of ATP synthesis and altered ratio of doubling time in galactose *versus* glucose in both cell types. We also transferred mutation m.9008C>G because their telomerase transduction had failed and primary fibroblasts had presented with altered proliferation in galactose. As pathological controls, we transferred the three confirmed mutations that had been analyzed in several independent fibroblast lines (m.8993T>C, m.8993T>G and m.9185T>C). As controls, we transferred mutation m.8648G>A that had not shown any anomaly in fibroblasts. We also used 12 different cybrid clones with wild type sequence, obtained during the diverse fusion experiments. PCR-restriction showed that all the mutant cybrid clones had homoplasmic level of the transferred mutation while all controls were homoplasmic for the wild type sequence (Figure e-1).

Among the cybrids with confirmed deleterious mutations, only those with the severe m.8993T>G mutation presented with an abnormal ATP production rate (Figure 4A). That defective ATP production was associated with significant defect of ATP synthase and combined defect of respiratory complexes I and IV (Figure 4B to 4F). In contrast, cybrids with homoplasmic confirmed m.8993T>C or m.9195T>C mutation did not show any significant anomaly of their ATP production rate, OXPHOS activities or doubling time in galactose *versus* glucose, showing the relative stringency of these parameters used for the detection of a complex V defect. We thus measured lactate production, which appeared a sensitive parameter in a previous report (Frey et al., 2017). Lactate production in 5 mM glucose was abnormally high in all cybrid lines with a confirmed deleterious mutation, confirming the sensitivity of that parameter (Figure 3H).

As expected when choosing them as controls, cybrids with the m.8648G>A mutation had normal results. In contrast, three cybrid lines with putative mutations presented with significant anomalies showing the mtDNA origin of the defects observed in fibroblasts. Table e-5 describes the clinical history of the patients with these three mutations. Cybrids with the m.8424T>C mutation presented with the most severe defect with consequences identical to those induced by the confirmed m.8993T>G mutation. Cybrids with the m.8975T>C mutation presented with combined defect of complexes I+IV but not of ATP synthase or ATP production. Cybrids with the m.9006C>G mutation did not present with any significant defect of OXPHOS activities but showed moderately low ATP production. All cybrids with abnormal ATP production and/or OXPHOS activities had abnormal growth in galactose *versus* glucose, showing the functional relevance of the observed defects (Figure 4G). Cybrids with m.8993T>G and m.8424T>C mutations almost stopped growing in galactose, preventing reliable calculation of their doubling time. We therefore compared their growth in 5 mM glucose to that in 22.5mM glucose instead of comparing galactose to glucose medium. Western blot analysis of cybrids proteins confirmed that mutations m.8424T>C and m.8993T>G had a global impact on respiratory complexes I and IV (Figure e-3). Cybrids with mutation m.8975T>C presented with a peculiar pattern associating a significant increase of MT-ATP6 subunit with significant decrease of CO2, a complex IV catalytic subunit. That pattern corresponded to the activity pattern observed in these cells, associating normal complex V-linked ATP hydrolysis with severe complex IV defect (see Figure 4). Complex V-linked ATP hydrolysis activity of cybrids tightly correlated with MT-ATP6 steady state and more loosely to ATPF1B. In accordance with the significant impact of complex V defect on respiratory complexes in cybrids, complex V activity tightly correlated with the steady state amount of ND1 and CO2 subunits.
The cybrids with the m.8424T>C mutation were particularly interesting because of their highly variable ATP production rate (Figure 4A). That variation appeared essentially due to one cybrid line (number 38) (Figure e-4). Despite the presence of homoplasmic levels of the m.8424T>C mutation in all cybrid clones (Figure e-1), the clone 38 maintained both its ATP production and the activity

of complexes V, I and IV (Figure e-4A to 3D). In contrast, all these parameters were defective in three other clones (clones 1, 31 and 33). The high levels of complex II and citrate synthase activities in clone 38 *versus* clones 1, 31 and 33 suggested that mitochondrial proliferation could be the involved compensatory mechanism in clone 38 (Figure e-4E to 3F). Compensation seemed to be efficient on clone 38 ratio of doubling time but the small number of assays (only one for clones 1, 31 and 33, two for clone 38) prevented statistical analysis (Figure e-4G). In contrast, lactate production of clone 38 remained increased similarly to that of clone 1 and 31 (Figure e-4H).

3.3 Structure-function relationships

The 3D structure of mammalian complex V has been determined at an atomic resolution, allowing precise localization of mutated residues. To examine their possible role in the catalytic mechanism, we localized the five mutations analyzed up to cybrids (Figure 5). Mutated residues involved subunit 6 (also called "subunit a") and subunit 8, both located in the membranous part of the ATP synthase stator. Subunit a interacts with the ring of subunits c, which, coupled with transmembrane proton flow, rotates clockwise (view from the matrix) during ATP hydrolysis and counter-clockwise during ATP synthesis. During ATP synthesis, subunit a transfers protons from the intermembrane space to the c-ring and from the c-ring to the matrix. The opposite occurs during ATP hydrolysis. During the process, every c subunit transiently binds a proton on its glutamate 58, located on a transmembrane α-helix, in the middle of the membrane, and facing subunit a. Subunit 8 is not involved in the catalytic proton transfer, because it is remote from the c-ring. It forms an α-helix, spanning the membrane and protruding in the matrix. It is associated with other subunits that constitute the stator.

Among the confirmed deleterious mutations, the most severe mutation here considered, m8993T>G, substitutes an arginine for leucine 156 of subunit a. In the bovine structural model, strictly homologous to the human one in this region, Leu156 is located in the fifth α-helix (P139-L181) of subunit a. It closely interacts with glutamate 58 of one subunit c (Figure 5 C-D). It is also adjacent to Arg159, which plays a key electrostatic role in the proton transfer (Mitome et al., 2010).

Introduction of an additional positive charge in this critical interfacial region most certainly disturbs the proton transfer. The less severe mutation m.8993T>C, which substitutes a proline for leucine 156, has no electrostatic effect, but it can indirectly and moderately affect the proton transfer by distorting the fifth α-helix of subunit a. Mutation m.9185T>C also substitutes a proline for a leucine at position 220. Leu220 is located at the extremity of the sixth α-helix (A189-Y221) of subunit a, which is antiparallel to the fifth α-helix interacting with the c-ring (Figure 5C). Since Leu220 is located far from the a-c interface, the mutation cannot directly disturb the proton transfer. However, it may change the orientation of the sixth α-helix in such a way that it affects the movement of the rotor, for example by touching the c-ring.

Among the putative mutations, mutation m.8424T>C substitutes a proline to Leu20 in subunit 8 in the region that mainly interacts with subunit a, Leu20 itself being close to Met25 and Phe78 of subunit a. It is conceivable that the Leu20Pro mutation distorts the α-helix of subunit 8 in such a way that it affects the complex assembly or its stability. Mutation m.8975T>C substitutes a proline for Leu150 of subunit a. In the bovine enzyme, a phenylalanine replaces Leu150, indicating that the aminoacid precise identity is not crucial. However, Leu 150 is located in the fifth α-helix of subunit a, not far from Leu156. Its mutation into a proline could affect the proton transfer through a distortion of the α-helix, as already proposed for the Leu156Pro mutation. Finally, the mechanism by which mutation m.9008C>G could affect complex V activity is not obvious. Its substitutes a serine for Thr161. Thr161 is conserved in mammals but not in yeast, where it is replaced by a glycine. It is located in the fifth α-helix, on the side opposite to that interacting with the c-ring. It is not expected to significantly distort the α-helix and, since this region does not interact with other subunits, an effect in protein assembly or stability also seems to be ruled out.

4 Discussion

4.1 Cybrids analyses demonstrated the deleterious nature of three MT-ATP6/8 mutations

The main interest of the cybrid approach is to demonstrate the mtDNA responsibility on any OXPHOS defect co-transferred with the patients' mtDNA. It is considered a "gold-standard" for ascribing a deleterious nature to mtDNA mutations (Yarham et al., 2011).

Obviously, variants co-transferred with the *MT-ATP6/*8 mutations could have a role in the OXPHOS defect. In the case of mutations m.8424T>C or m.9008C>G, none of the co-transferred mtDNA variants had any potential deleterious impact as evaluated by prediction software (Table e-4). Mutation m.8975T>C was initially associated in muscle with two heteroplasmic mutations. One, affecting 10% mtDNA molecules, was present but prediction software unanimously considered that mutation as non-deleterious. The second was the known deleterious *MT-TL1* m.3243A>G MELAS mutation, affecting 65% mtDNA molecules of muscle. We ruled out the presence of the MELAS mutation in the cybrids DNA using restriction-PCR and thus could ascribe the observed effect in cybrids to mutation m.8975T>C (Figure e-1).

In conclusion, cybrids analyses demonstrated the deleterious nature of mutations m.8424T>C, m.8975T>C and m.9008C>G by showing their association with increased glycolysis and reduced growth in galactose (the three mutations), defective respiratory complexes activity (the first two mutations), and decreased complex V-linked ATP hydrolysis (mutation m.8424T>C).

4.2 Graded consequences of deleterious MT-ATP6/8 mutations in cybrids

In the clinical field, the patients' nuclear genetic background might significantly modify the consequences of the mtDNA mutation. Because cybrids share a common nuclear DNA from the parental rho0 sarcoma line, one assumed that the mutations themselves induced the variable consequences observed in cybrids. We thus could define four grades in the severity of the mutations functional impact. The minimal consequence was the increased glycolysis, observed in cybrids with the confirmed mutations m.8993T>C and m.9185T>C. It associated poor growth in galactose in the second level of severity (mutation m.9008C>G). Addition of combined defect of respiratory complexes I and IV defined the third grade of severity (mutation 8975T>C) while the occurrence of defect in complex V-linked ATP hydrolysis defined the most severe mutations (m.8993T>G and

m.8424T>C). Of note, we did not analyze complex III in cybrids because of the limited amount of samples but also because that assay has relatively large standard deviation in control samples, leading to difficult demonstration of partial defects (Medja et al., 2009).

The graded consequences of complex V defects have direct consequences on their diagnosis. Complex V-linked ATP hydrolysis, the sole assay completely specific for complex V, was the least sensitive parameter, being defective only with the two most severe mutations (m.8993T>G and m.8424T>C). At the opposite, the two most sensitive parameters (increased glycolysis and poor growth in galactose) lacked specificity because their cause could be any OXPHOS alteration. ATP production rate was in an intermediary position. It was relatively specific for complex V because it used several substrates, oxidized by different enzymes and entering the respiratory chain at the level of complex I or complex II. However, it showed poor sensitivity because of the large variation observed between experiments on the same cells. The literature reported several different protocols for the measurement of ATP production in cybrids (Vojtiskova et al., 2004, Cortes-Hernandez et al., 2007, Vazquez-Memije et al., 2009, Auré et al., 2013, Hejzlarova et al., 2015). Their relative sensitivity and relevance to cell physiology would be important to evaluate with respect to diagnosis. In our work, we chose to avoid mitochondrial preparation because its very small yield in cells might introduce an important bias. We also chose to use a very short incubation time (4 minutes) and multiple substrates (pyruvate, glutamate and succinate), both conditions being close to cellular physiology.

Comparison of our results in cybrids with reported similar analyses could only apply to the three confirmed mutations (Trounce et al., 1994, Cortes-Hernandez et al., 2007, Rak et al., 2007, Kucharczyk et al., 2009, Vazquez-Memije et al., 2009, Auré et al., 2013, Kabala et al., 2014). It was complicated by the different models (yeast or cybrids), by the different set of analyses (ATP production, complex V-linked ATP hydrolysis, OXPHOS analysis), and by the often-different protocols applied for each analysis. For a same mutation, yeast always had lower ATP production rate than cybrids (Cortes-Hernandez et al., 2007, Rak et al., 2007, Kucharczyk et al., 2009,

Vazquez-Memije et al., 2009). In the case of mutation m.8993T>G or T>C, yeast presented with associated respiratory complex IV defect, an observation reminiscent of our findings in cybrids with m.8993T>G, m.8244T>T and m.8975T>C mutation (Rak et al., 2007, Kucharczyk et al., 2009). There is no similar spectrophotometric analysis of respiratory complexes in cybrids in the literature (Cortes-Hernandez et al., 2007, Vazquez-Memije et al., 2009). On the other hand, complex V-linked ATP hydrolysis showed discrepancy, for example being decreased in fibroblasts but normal in cybrids with the m.8993T>G mutation (Vazquez-Memije et al., 2009). In that particular case, the assay used isolated mitochondria, which are difficult to purify from cell cultures in a reproducible manner, and a medium devoid of magnesium, an essential ion for complex V activity. We believe that the protocol we used in our study brought significant improvement in the spectrophotometric analysis of complex V activity because its assay medium was based on the in-depth analysis of complex V assay in different tissues (Haraux and Lombes, 2019) and because it used whole cell pellets that were submitted to osmotic choc and sonication. However, even with that protocol, oligomycin-sensitive complex V-linked ATP hydrolysis appeared poorly sensitive, being defective only with the most severe mutations.

Cybrid clone 38 with homoplasmic levels of the m.8424T>C mutation brought a very interesting observation when it showed compensation for the deleterious impact of mutation m.8424T>C through increased mitochondrial biogenesis, an important compensatory mechanism that has been already extensively studied up to clinical trials (El-Hattab et al., 2017). The parental rho0 143B line derived from a pediatric osteosarcoma, a tumor characterized by the presence of numerous, often unstable, chromosomal rearrangements (Bayani et al., 2003, Squire et al., 2003). Its nuclear DNA instability could allow screening for potential compensatory mechanisms relevant for therapeutic strategy.

In conclusion, taking together the data from the literature and those obtained in the present study, analyses of cybrids unambiguously disclose only the most severe *MT-ATP6/8* mutations. The gradation of the mutations functional impact imposes to apply complementary functional analyses

with various sensitivity/specificity. In their absence, under-diagnosis of the deleterious nature of *MT-ATP6/8* mutations is likely. We did not analyze in cybrids six of the mutations with a maximal score with pathogenicity prediction. Those mutations thus remained with a disputable status with respect to their role in the disease. We could not perform that analysis in the absence of fibroblasts for three of these mutations (m.8639T>C, m.8969G>C and m.8999T>C). More importantly, for the three remaining mutations (m.8403T>C, m.8382C>T and m.9086C>T), we had decided against obtaining cybrids because of the results close to normal of fibroblasts analysis. Now, with the benefit of hindsight on the very graded consequences of the mutations, we think that these three mutations are worth their analysis in cybrids.

4.3 Variation between tissues of the consequences of deleterious MT-ATP6/8 mutations

Muscle, fibroblasts and cybrids, all with homoplasmic mutation, disclosed striking differences in the consequences of the complex V. Muscle appeared less prone to compensation than cells. Indeed, in the case of mutations m.8382C>T and m.9035T>C, muscle presented with significant defect of complex V-linked ATP hydrolysis and associated complex I defect whereas cells had normal normal ATP production and OXPHOS activities. We never observed the reverse situation. Obtaining muscle fragment thus appeared essential for the diagnosis of complex V defect.

With respect to diagnosis, fibroblasts appeared the worst tissue as they showed very little impact of deleterious *MT-ATP6/8* mutations. In addition, transduction with the catalytic subunit of telomerase erased most abnormal parameters observed in the primary fibroblasts, suggesting that the few observed anomalies were due to early senescence. Normal citrate synthase and complex II activity of fibroblasts excluded an increased mitochondrial biogenesis responsible for the compensation. In accordance with the little impact observed in our study, only two severe mutations, both associated with early-onset phenotypes, had reported consequences in fibroblasts. Mutation m.8993T>G induced catalytic dysfunction, decreased assembly of complex V, instability of the assembled complex V and increased oxygen reactive species production (Houstek et al., 1995, Nijtmans et al., 2001, Vojtiskova et al., 2004, Mracek et al., 2006, Cortes-Hernandez et al., 2007). Mutation

m.9205delTA was associated with normal complex V-linked ATP hydrolysis but defective respiratory complex IV, a pattern reminiscent of our observations with mutation m.8975T>C (Seneca et al., 1996, Temperley et al., 2003, Jesina et al., 2004).

4.4 Relationship between complex V defect and respiratory chain

The defect of respiratory complexes associated with complex V defects was an important finding in our study. It could prevent a proper diagnosis because it occurred before a significant decrease of the complex V-linked ATP hydrolysis. Its mechanisms are at present unknown, possibly multiple, from an altered stability of complex V modifying the supercomplexes steady state to bioenergetics consequences of the complex V deficiency including oxidative stress and decreased ATP availability. These mechanisms might differ between tissues. For example, disrupting the dimeric assembly of complex V in HeLa cells by downregulating the expression of accessory subunits e or g led to severe OXPHOS disorganization in human cells but not in yeast (Habersetzer et al., 2013). Among the bioenergetics consequences of complex V defects, oxidative stress could target the respiratory complexes and decrease their stability. On the other hand, decreased ATP availability could modify the transcription/translation/quality control of respiratory complexes subunits. It could also modify complex V post-translational modifications that we recently proposed to modulate complex V catalytic efficacy in muscle, heart, liver and brain (Haraux and Lombes, 2019).

4.5 Genotype/phenotype relationship

The complex pathophysiology of the diverse *MT-ATP6/8* mutations and the ensuing multiple potential compensatory mechanisms most probably underlie their complex genotype/phenotype relationship. Defective complex V activity and ATP production were obvious consequences initially proposed to explain the severe, early-onset, presentations of *MT-ATP6/8* mutations including encephalopathies (non-specific with seizures (Seneca et al., 1996) or with basal ganglia involvement defining Leigh syndrome (Holt et al., 1990)) and cardiomyopathy (often with cardiac failure) (Ware et al., 2009). The similar presentation encountered with recessive *TMEM* mutations inducing defective complex V assembly (Cizkova et al., 2008) strengthened that hypothesis.

However, a severely defective ATP production could not fit with the mild phenotypes with adult-onset that were later associated with homoplasmic levels of some of the mutations initially observed with early-onset clinical presentations. These phenotypes were neurological (spinocerebellar syndrome (Rantamaki et al., 2005, Verny et al., 2010, Pfeffer et al., 2012), isolated peripheral neuropathy (Pitceathly et al., 2012, Synofzik et al., 2012) or episodic paralysis (Auré et al., 2013)) but did not include encephalopathy or heart failure. These clinical differences suggested that efficient compensation and/or alternative deleterious consequences could exist in heart and brain but not in peripheral nerves or skeletal muscle.

The lack of any mitochondrial proliferation in muscle suggested that increased mitochondrial biogenesis was not a likely compensatory mechanism, in contrast to the observation in clone cybrid 38 with the m.8424T>C mutation.

Among the bioenergetics consequences of complex V defect, oxidative stress would allow for phenotypic variability through individual capacity of quenching or quality control (Mracek et al., 2006). It could underlie the presence of the additional deleterious mtDNA mutation (MELAS m.3243A>G) in the patient with the m.8975T>C mutation in the present study, a situation already encountered for another MELAS mutation (m.3271T>C) in a large pedigree with the *MT-ATP6* m.9185T>C mutation and episodic paralysis (Auré et al., 2013).

Whatever the underlying compensatory mechanisms, it is remarkable that the families with a mild phenotype included patients belonging to successive generations (Rantamaki et al., 2005, Craig et al., 2007, Verny et al., 2010, Pfeffer et al., 2012, Pitceathly et al., 2012, Synofzik et al., 2012, Auré et al., 2013). In contrast, families with severe early-onset disease were constantly small (Holt et al., 1990, Campos et al., 1997, Moslemi et al., 2005, Morava et al., 2006, Castagna et al., 2007, Childs et al., 2007). That observation suggested that the nuclear background underlying compensation involved common genetic trait(s).

5 Conclusion

Systematic sequencing of *MT-ATP6/8* genes in adult patients with a suspicion of mitochondrial diseases disclosed 3.4% confirmed mutations (5/144 variants, affecting 15/512 patients) and 18.8% putative mutations (27/144 variants), among which we demonstrated three as deleterious in cybrids. Functional analysis of deleterious *MT-ATP6/8* mutations disclosed striking gradation in severity and tissue-specific responses, with muscle being more informative than fibroblasts and early secondary respiratory defect.

Under-diagnosis of deleterious *MT-ATP6/8* mutations, especially in adult patients, appeared likely because of the complexity and tissue-specificity of their induced consequences, in addition to the lack of characteristic histological mitochondrial hallmarks.

Acknowledgements

The authors thank the AFM Myobank, Institut de Myologie, for providing human control muscle and fibroblasts samples and for the repository of cell lines.

Funding: This work was supported by the Fondation pour la Recherche Médicale (FRM-grant DPM20121125550 to AL), the AFM Telethon and the AMMi. The funders had no role in study design, data collection and analysis, decision to publish, or preparation of the manuscript..

References

Andrews, R. M., Kubacka, I., Chinnery, P. F., Lightowlers, R. N., Turnbull, D. M. and Howell, N., 1999. Reanalysis and revision of the Cambridge reference sequence for human mitochondrial DNA. Nat Genet 23(2): 147.

Auré, K., Dubourg, O., Jardel, C., Clarysse, L., Sternberg, D., Fournier, E., Laforet, P., Streichenberger, N., Petiot, P., Gervais-Bernard, H., Vial, C., Bedat-Millet, A. L., Drouin-Garraud, V., Bouillaud, F., Vandier, C., Fontaine, B. and Lombès, A., 2013. Episodic weakness due to mitochondrial DNA MT-ATP6/8 mutations. Neurology 81(21): 1810-1818.

Auré, K., Mamchaoui, K., Frachon, P., Butler-Browne, G. S., Lombès, A. and Mouly, V., 2007. Impact on oxidative phosphorylation of immortalization with the telomerase gene. Neuromuscul Disord 17: 368-375.

Barca, E., Ganetzky, R. D., Potluri, P., Juanola-Falgarona, M., Gai, X., Li, D., Jalas, C., Hirsch, Y., Emmanuele, V., Tadesse, S., Ziosi, M., Akman, H. O., Chung, W. K., Tanji, K., McCormick, E. M., Place, E., Consugar, M., Pierce, E. A., Hakonarson, H., Wallace, D. C., Hirano, M. and Falk, M. J., 2018. USMG5 Ashkenazi Jewish founder mutation impairs mitochondrial complex V dimerization and ATP synthesis. Hum Mol Genet 27(19): 3305-3312.

Barthélémy, C., Ogier de Baulny, H., Diaz, J., Cheval, M. A., Frachon, P., Romero, N., Goutieres, F., Fardeau, M. and Lombès, A., 2001. Late-onset mitochondrial DNA depletion: DNA copy number, multiple deletions, and compensation. Ann Neurol 49(5): 607-617.

Bayani, J., Zielenska, M., Pandita, A., Al-Romaih, K., Karaskova, J., Harrison, K., Bridge, J. A., Sorensen, P., Thorner, P. and Squire, J. A., 2003. Spectral karyotyping identifies recurrent complex rearrangements of chromosomes 8, 17, and 20 in osteosarcomas. Genes Chromosomes Cancer 36(1): 7-16.

Campos, Y., Martin, M. A., Rubio, J. C., Solana, L. G., Garcia-Benayas, C., Terradas, J. L. and Arenas, J., 1997. Leigh syndrome associated with the T9176C mutation in the ATPase 6 gene of mitochondrial DNA. Neurology 49(2): 595-597.

Carrozzo, R., Tessa, A., Vazquez-Memije, M. E., Piemonte, F., Patrono, C., Malandrini, A., Dionisi-Vici, C., Vilarinho, L., Villanova, M., Schagger, H., Federico, A., Bertini, E. and Santorelli, F. M., 2001. The T9176G mtDNA mutation severely affects ATP production and results in Leigh syndrome. Neurology 56(5): 687-690.

Castagna, A. E., Addis, J., McInnes, R. R., Clarke, J. T., Ashby, P., Blaser, S. and Robinson, B. H., 2007. Late onset Leigh syndrome and ataxia due to a T to C mutation at bp 9,185 of mitochondrial DNA. Am J Med Genet A 143A(8): 808-816.

Childs, A. M., Hutchin, T., Pysden, K., Highet, L., Bamford, J., Livingston, J. and Crow, Y. J., 2007. Variable phenotype including Leigh syndrome with a 9185T>C mutation in the MTATP6 gene. Neuropediatrics 38(6): 313-316.

Chretien, D., Bourgeron, T., Rötig, A., Munnich, A. and Rustin, P., 1990. The measurement of the rotenone-sensitive NADH cytochrome c reductase activity in mitochondria isolated from minute amount of human skeletal muscle. Biochem.Biophys.Res.Comm. 173(1): 26-33.

Cizkova, A., Stranecky, V., Mayr, J. A., Tesarova, M., Havlickova, V., Paul, J., Ivanek, R., Kuss, A. W., Hansikova, H., Kaplanova, V., Vrbacky, M., Hartmannova, H., Noskova, L., Honzik, T., Drahota, Z., Magner, M., Hejzlarova, K., Sperl, W., Zeman, J., Houstek, J. and Kmoch, S., 2008. TMEM70 mutations cause isolated ATP synthase deficiency and neonatal mitochondrial encephalocardiomyopathy. Nat Genet 40(11): 1288-1290.

Cortes-Hernandez, P., Vazquez-Memije, M. E. and Garcia, J. J., 2007. ATP6 homoplasmic mutations inhibit and destabilize the human F1F0-ATP synthase without preventing enzyme assembly and oligomerization. J Biol Chem 282(2): 1051-1058.

Craig, K., Elliott, H. R., Keers, S. M., Lambert, C., Pyle, A., Graves, T. D., Woodward, C., Sweeney, M. G., Davis, M. B., Hanna, M. G. and Chinnery, P. F., 2007. Episodic ataxia and hemiplegia caused by the 8993T->C mitochondrial DNA mutation. J Med Genet 44(12): 797-799.

Dautant, A., Meier, T., Hahn, A., Tribouillard-Tanvier, D., di Rago, J. P. and Kucharczyk, R., 2018. ATP Synthase Diseases of Mitochondrial Genetic Origin. Front Physiol 9: 329.

De Meirleir, L., Seneca, S., Lissens, W., De Clercq, I., Eyskens, F., Gerlo, E., Smet, J. and Van Coster, R., 2004. Respiratory chain complex V deficiency due to a mutation in the assembly gene ATP12. J Med Genet 41(2): 120-124.

El-Hattab, A. W., Zarante, A. M., Almannai, M. and Scaglia, F., 2017. Therapies for mitochondrial diseases and current clinical trials. Mol Genet Metab 122(3): 1-9.

Frey, S., Geffroy, G., Desquiret-Dumas, V., Gueguen, N., Bris, C., Belal, S., Amati-Bonneau, P., Chevrollier, A., Barth, M., Henrion, D., Lenaers, G., Bonneau, D., Reynier, P. and Procaccio, V.,

2017. The addition of ketone bodies alleviates mitochondrial dysfunction by restoring complex I assembly in a MELAS cellular model. Biochim Biophys Acta Mol Basis Dis 1863(1): 284-291.

Gorman, G. S., Chinnery, P. F., DiMauro, S., Hirano, M., Koga, Y., McFarland, R., Suomalainen, A., Thorburn, D. R., Zeviani, M. and Turnbull, D. M., 2016. Mitochondrial diseases. Nat Rev Dis Primers 2: 16080.

Gorman, G. S., Schaefer, A. M., Ng, Y., Gomez, N., Blakely, E. L., Alston, C. L., Feeney, C., Horvath, R., Yu-Wai-Man, P., Chinnery, P. F., Taylor, R. W., Turnbull, D. M. and McFarland, R., 2015. Prevalence of nuclear and mitochondrial DNA mutations related to adult mitochondrial disease. Ann Neurol 77(5): 753-759.

Habersetzer, J., Larrieu, I., Priault, M., Salin, B., Rossignol, R., Brethes, D. and Paumard, P., 2013. Human F1F0 ATP synthase, mitochondrial ultrastructure and OXPHOS impairment: a (super-)complex matter? PLoS One 8(10): e75429.

Haraux, F. and Lombes, A., 2019. Kinetic analysis of ATP hydrolysis by complex V in four murine tissues: Towards an assay suitable for clinical diagnosis. PLoS One 14(8): e0221886.

Havlickova, V., Kaplanova, V., Nuskova, H., Drahota, Z. and Houstek, J., 2010. Knockdown of F1 epsilon subunit decreases mitochondrial content of ATP synthase and leads to accumulation of subunit c. Biochim Biophys Acta 1797(6-7): 1124-1129.

Hejzlarova, K., Kaplanova, V., Nuskova, H., Kovarova, N., Jesina, P., Drahota, Z., Mracek, T., Seneca, S. and Houstek, J., 2015. Alteration of structure and function of ATP synthase and cytochrome c oxidase by lack of Fo-a and Cox3 subunits caused by mitochondrial DNA 9205delTA mutation. Biochem J 466(3): 601-611.

Hejzlarova, K., Mracek, T., Vrbacky, M., Kaplanova, V., Karbanova, V., Nuskova, H., Pecina, P. and Houstek, J., 2014. Nuclear genetic defects of mitochondrial ATP synthase. Physiol Res 63 Suppl 1: S57-71.

Hernandez-Segura, A., Nehme, J. and Demaria, M., 2018. Hallmarks of Cellular Senescence. Trends Cell Biol 28(6): 436-453.

Holt, I. J., Harding, A. E., Petty, R. K. H. and Morgan-Hughes, J. A., 1990. A new mitochondrial disease associated with mitochondrial DNA heteroplasmy. Am.J.Hum.Genet. 46: 428-433.

Houstek, J., Klement, P., Hermanska, J., Houstkova, H., Hansikova, H., Van den Bogert, C. and Zeman, J., 1995. Altered properties of mitochondrial ATP-synthase in patients with a T-->G mutation in the ATPase 6 (subunit a) gene at position 8993 of mtDNA. Biochim Biophys Acta 1271(2-3): 349-357.

Jesina, P., Tesarova, M., Fornuskova, D., Vojtiskova, A., Pecina, P., Kaplanova, V., Hansikova, H., Zeman, J. and Houstek, J., 2004. Diminished synthesis of subunit a (ATP6) and altered function of ATP synthase and cytochrome c oxidase due to the mtDNA 2 bp microdeletion of TA at positions 9205 and 9206. Biochem J 383(Pt. 3): 561-571.

Jonckheere, A. I., Renkema, G. H., Bras, M., van den Heuvel, L. P., Hoischen, A., Gilissen, C., Nabuurs, S. B., Huynen, M. A., de Vries, M. C., Smeitink, J. A. and Rodenburg, R. J., 2013. A complex V ATP5A1 defect causes fatal neonatal mitochondrial encephalopathy. Brain 136(Pt 5): 1544-1554.

Kabala, A. M., Lasserre, J. P., Ackerman, S. H., di Rago, J. P. and Kucharczyk, R., 2014. Defining the impact on yeast ATP synthase of two pathogenic human mitochondrial DNA mutations, T9185C and T9191C. Biochimie 100: 200-206.

King, M. P. and Attardi, G., 1989. Human cells lacking mtDNA: repopulation with exogenous mitochondria by complementation. Science 246(4929): 500-503.

Kogelnik, A. M., Lott, M. T., Brown, M. D., Navathe, S. B. and Wallace, D. C., 1997. MITOMAP : an update on the status of the human mitochondrial genome database. Nucl. Acids Res. 25: 196-199.

Kucharczyk, R., Ezkurdia, N., Couplan, E., Procaccio, V., Ackerman, S. H., Blondel, M. and di Rago, J. P., 2010. Consequences of the pathogenic T9176C mutation of human mitochondrial DNA on yeast mitochondrial ATP synthase. Biochim Biophys Acta 1797(6-7): 1105-1112.

Kucharczyk, R., Rak, M. and di Rago, J. P., 2009. Biochemical consequences in yeast of the human mitochondrial DNA 8993T>C mutation in the ATPase6 gene found in NARP/MILS patients. Biochim Biophys Acta 1793(5): 817-824.

Manfredi, G., Gupta, N., Vazquez-Memije, M. E., Sadlock, J. E., Spinazzola, A., De Vivo, D. C. and Schon, E. A., 1999. Oligomycin induces a decrease in the cellular content of a pathogenic mutation in the human mitochondrial ATPase 6 gene. J Biol Chem 274(14): 9386-9391.

Mayr, J. A., Havlickova, V., Zimmermann, F., Magler, I., Kaplanova, V., Jesina, P., Pecinova, A., Nuskova, H., Koch, J., Sperl, W. and Houstek, J., 2010. Mitochondrial ATP synthase deficiency due to a mutation in the ATP5E gene for the F1 epsilon subunit. Hum Mol Genet 19(17): 3430-3439.

Medja, F., Allouche, S., Frachon, P., Jardel, C., Malgat, M., de Camaret, B. M., Slama, A., Lunardi, J., Mazat, J. P. and Lombes, A., 2009. Development and implementation of standardized respiratory chain spectrophotometric assays for clinical diagnosis. Mitochondrion 9(5): 331-339.

Meulemans, A., Seneca, S., Pribyl, T., Smet, J., Alderweirldt, V., Waeytens, A., Lissens, W., Van Coster, R., De Meirleir, L., di Rago, J. P., Gatti, D. L. and Ackerman, S. H., 2010. Defining the pathogenesis of the human Atp12p W94R mutation using a Saccharomyces cerevisiae yeast model. J Biol Chem 285(6): 4099-4109.

Mitome, N., Ono, S., Sato, H., Suzuki, T., Sone, N. and Yoshida, M., 2010. Essential arginine residue of the F(o)-a subunit in F(o)F(1)-ATP synthase has a role to prevent the proton shortcut without c-ring rotation in the F(o) proton channel. Biochem J 430(1): 171-177.

Morava, E., Rodenburg, R. J., Hol, F., de Vries, M., Janssen, A., van den Heuvel, L., Nijtmans, L. and Smeitink, J., 2006. Clinical and biochemical characteristics in patients with a high mutant load of the mitochondrial T8993G/C mutations. Am J Med Genet A 140(8): 863-868.

Moslemi, A. R., Darin, N., Tulinius, M., Oldfors, A. and Holme, E., 2005. Two new mutations in the MTATP6 gene associated with Leigh syndrome. Neuropediatrics 36(5): 314-318.

Mracek, T., Pecina, P., Vojtiskova, A., Kalous, M., Sebesta, O. and Houstek, J., 2006. Two components in pathogenic mechanism of mitochondrial ATPase deficiency: energy deprivation and ROS production. Exp Gerontol 41(7): 683-687.

Nijtmans, L. G., Henderson, N. S., Attardi, G. and Holt, I. J., 2001. Impaired ATP Synthase Assembly Associated with a Mutation in the Human ATP Synthase Subunit 6 Gene. J Biol Chem 276(9): 6755-6762.

Olahova, M., Yoon, W. H., Thompson, K., Jangam, S., Fernandez, L., Davidson, J. M., Kyle, J. E., Grove, M. E., Fisk, D. G., Kohler, J. N., Holmes, M., Dries, A. M., Huang, Y., Zhao, C., Contrepois, K., Zappala, Z., Fresard, L., Waggott, D., Zink, E. M., Kim, Y. M., Heyman, H. M., Stratton, K. G., Webb-Robertson, B. M., Undiagnosed Diseases, N., Snyder, M., Merker, J. D., Montgomery, S. B., Fisher, P. G., Feichtinger, R. G., Mayr, J. A., Hall, J., Barbosa, I. A., Simpson, M. A., Deshpande, C., Waters, K. M., Koeller, D. M., Metz, T. O., Morris, A. A., Schelley, S., Cowan, T., Friederich, M. W., McFarland, R., Van Hove, J. L. K., Enns, G. M., Yamamoto, S., Ashley, E. A., Wangler, M. F., Taylor, R. W., Bellen, H. J., Bernstein, J. A. and Wheeler, M. T., 2018. Biallelic Mutations in ATP5F1D, which Encodes a Subunit of ATP Synthase, Cause a Metabolic Disorder. Am J Hum Genet 102(3): 494-504.

Pfeffer, G., Blakely, E. L., Alston, C. L., Hassani, A., Boggild, M., Horvath, R., Samuels, D. C., Taylor, R. W. and Chinnery, P. F., 2012. Adult-onset spinocerebellar ataxia syndromes due to MTATP6 mutations. J Neurol Neurosurg Psychiatry 83(9): 883-886.

Pitceathly, R. D., Murphy, S. M., Cottenie, E., Chalasani, A., Sweeney, M. G., Woodward, C., Mudanohwo, E. E., Hargreaves, I., Heales, S., Land, J., Holton, J. L., Houlden, H., Blake, J., Champion, M., Flinter, F., Robb, S. A., Page, R., Rose, M., Palace, J., Crowe, C., Longman, C., Lunn, M. P., Rahman, S., Reilly, M. M. and Hanna, M. G., 2012. Genetic dysfunction of MT-ATP6 causes axonal Charcot-Marie-Tooth disease. Neurology 79(11): 1145-1154.

Rak, M., Tetaud, E., Duvezin-Caubet, S., Ezkurdia, N., Bietenhader, M., Rytka, J. and di Rago, J. P., 2007. A yeast model of the neurogenic ataxia retinitis pigmentosa (NARP) T8993G mutation in the mitochondrial ATP synthase-6 gene. J Biol Chem 282(47): 34039-34047.

Rantamaki, M. T., Soini, H. K., Finnila, S. M., Majamaa, K. and Udd, B., 2005. Adult-onset ataxia and polyneuropathy caused by mitochondrial 8993T-->C mutation. Ann Neurol 58(2): 337-340.

Repetto, G., del Peso, A. and Zurita, J. L., 2008. Neutral red uptake assay for the estimation of cell viability/cytotoxicity. Nat Protoc 3(7): 1125-1131.

Sammut, I. A., Thorniley, M. S., Simpkin, S., Fuller, B. J., Bates, T. E. and Green, C. J., 1998. Impairment of hepatic mitochondrial respiratory function following storage and orthotopic transplantation of rat livers. Cryobiology 36(1): 49-60.

Seneca, S., Abramowicz, M., Lissens, W., Muller, M. F., Vamos, E. and de Meirleir, L., 1996. A mitochondrial DNA microdeletion in a newborn girl with transient lactic acidosis. J Inherit Metab Dis 19(2): 115-118.

Squire, J. A., Pei, J., Marrano, P., Beheshti, B., Bayani, J., Lim, G., Moldovan, L. and Zielenska, M., 2003. High-resolution mapping of amplifications and deletions in pediatric osteosarcoma by use of CGH analysis of cDNA microarrays. Genes Chromosomes Cancer 38(3): 215-225.

Synofzik, M., Schicks, J., Wilhelm, C., Bornemann, A. and Schols, L., 2012. Charcot-Marie-Tooth hereditary neuropathy due to a mitochondrial ATP6 mutation. Eur J Neurol 19(10): e114-116.

Temperley, R. J., Seneca, S. H., Tonska, K., Bartnik, E., Bindoff, L. A., Lightowlers, R. N. and Chrzanowska-Lightowlers, Z. M., 2003. Investigation of a pathogenic mtDNA microdeletion reveals a translation-dependent deadenylation decay pathway in human mitochondria. Hum Mol Genet 12(18): 2341-2348.

Thompson, K., Mai, N., Olahova, M., Scialo, F., Formosa, L. E., Stroud, D. A., Garrett, M., Lax, N. Z., Robertson, F. M., Jou, C., Nascimento, A., Ortez, C., Jimenez-Mallebrera, C., Hardy, S. A., He, L., Brown, G. K., Marttinen, P., McFarland, R., Sanz, A., Battersby, B. J., Bonnen, P. E., Ryan, M. T., Chrzanowska-Lightowlers, Z. M., Lightowlers, R. N. and Taylor, R. W., 2018. OXA1L

mutations cause mitochondrial encephalopathy and a combined oxidative phosphorylation defect. EMBO Mol Med 10(11).

Trounce, I., Neill, S. and Wallace, D. C., 1994. Cytoplasmic transfer of the mtDNA nt 8993 T-->G (ATP6) point mutation associated with Leigh syndrome into mtDNA-less cells demonstrates cosegregation with a decrease in state III respiration and ADP/O ratio. Proc Natl Acad Sci U S A 91(18): 8334-8338.

Vazquez-Memije, M. E., Rizza, T., Meschini, M. C., Nesti, C., Santorelli, F. M. and Carrozzo, R., 2009. Cellular and functional analysis of four mutations located in the mitochondrial ATPase6 gene. J Cell Biochem 106(5): 878-886.

Verny, C., Guegen, N., Desquiret, V., Chevrollier, A., Prundean, A., Dubas, F., Cassereau, J., Ferre, M., Amati-Bonneau, P., Bonneau, D., Reynier, P. and Procaccio, V., 2010. Hereditary spastic paraplegia-like disorder due to a mitochondrial ATP6 gene point mutation. Mitochondrion 11(1): 70-75.

Vojtiskova, A., Jesina, P., Kalous, M., Kaplanova, V., Houstek, J., Tesarova, M., Fornuskova, D., Zeman, J., Dubot, A. and Godinot, C., 2004. Mitochondrial membrane potential and ATP production in primary disorders of ATP synthase. Toxicol Mech Methods 14(1-2): 7-11.

Ware, S. M., El-Hassan, N., Kahler, S. G., Zhang, Q., Ma, Y. W., Miller, E., Wong, B., Spicer, R. L., Craigen, W. J., Kozel, B. A., Grange, D. K. and Wong, L. J., 2009. Infantile cardiomyopathy caused by a mutation in the overlapping region of mitochondrial ATPase 6 and 8 genes. J Med Genet 46(5): 308-314.

Yarham, J. W., Al-Dosary, M., Blakely, E. L., Alston, C. L., Taylor, R. W., Elson, J. L. and McFarland, R., 2011. A comparative analysis approach to determining the pathogenicity of mitochondrial tRNA mutations. Hum Mutat 32(11): 1319-1325.

Figure legends

Figure 1: Flowchart of the genetic analysis

The total number of variants (874) adds identical variants found in different patients. The subsequent categories only count different mutations and show the proportion of the initial variants falling into each category.

The nature of the mutation first separated the variants into missense and synonymous mutations. Three groups then separated the missense mutations. Known confirmed pathogenic mutations and recurrent polymorphisms did not require further analysis. Frequency of the mutation in GenBank sequences further divided the third category of missense mutations into two groups, with mutations reported more than 15 times considered as likely neutral variants. Prediction software, applied to the 30 last mutations, ruled out three mutations as probable neutral variants, leaving 27 mutations requiring direct analysis of their functional impact.

Figure 2: Functional analysis of primary fibroblasts with *MT-ATP6/8* mutations

A to G: Box-plot representation of rate of ATP production on OXPHOS substrates (A), complex V activity as measured with the oligomycin sensitive rate of ATP hydrolysis (B), complex I activity (C), complex II activity (D), complex IV activity (E), citrate synthase (F), and ratio of doubling time in glucose *versus* galactose (G) in primary fibroblasts. The mutation present in the diverse fibroblast lines is shown below the plots, with confirmed deleterious mutations in underlined characters. Each parameter was measured at least three times on independent biological samples with the exception of doubling time that was assayed only twice for fibroblasts with the 8382C>T or the 9086C>T mutation.

*, **, *** = $p<0.05$, 0.01, 0.001 respectively with two-sided comparison of mean (Mann and Whitney test unless Schapiro-Wilk test of normality permitted the use of a t test)

(H) Linear regression plot between the ratio of doubling time in galactose *versus* glucose and complex I (empty circles) or ATP production rate (black circles) observed in control primary fibroblasts; $p=0.103$ and 0.005 respectively using Spearman correlation test. Each dot represents the

median value of at least three measures on independent biological samples with the exception of one control with two measures of complex I and ATP production.

Figure 3: Functional analysis of fibroblasts with *MT-ATP6/8* mutations after their transduction with the telomerase catalytic subunit

(A) Spearman correlation plot between ATP production in fibroblasts transduced by telomerase and their primary counterpart. Each value is the median of three measures performed on independent cell preparations.

(B to H): Box-plot representation of rate of ATP production on OXPHOS substrates (B), complex V activity as measured with the oligomycin sensitive rate of ATP hydrolysis (C), complex I activity (D), complex II activity (E), complex IV activity (F), citrate synthase (G), and ratio of doubling time in glucose *versus* galactose (H) in fibroblasts transduced with the telomerase catalytic subunit. The mutation present in the diverse cell lines is shown below the plots, with confirmed deleterious mutations in underlined characters. Each parameter was measured at least two times on independent biological samples.

*, **, *** = $p<0.05$, 0.01, 0.001 respectively with two-sided comparison of mean (Mann and Whitney test unless Schapiro-Wilk test of normality permitted the use of a t test)

Figure 4: Functional analysis of cybrids with *MT-ATP6/8* mutations

A to H: Box-plot representation of rate of ATP production on OXPHOS substrates (A), complex V activity as measured with the oligomycin sensitive rate of ATP hydrolysis (B), complex I activity (C), complex II activity (D), complex IV activity (E), citrate synthase (F), ratio of doubling time in glucose *versus* galactose (G), and lactate production in cybrid clones. The mutation present in the diverse clones is shown below the plots, with confirmed deleterious mutations in underlined characters. Each parameter was measured at least four times on independent biological samples.

*, **, *** = $p<0.05$, 0.01, 0.001 respectively with two-sided comparison of mean (Mann and Whitney test unless Schapiro-Wilk test of normality permitted the use of a t test)

Figure 5: Structural model showing the position of the mutated residues in Complex V (ATP synthase).

Panels A-D: images obtained using the 3D-model of bovine mitochondrial ATP synthase (*pdb entry 5fij*) and the software Swiss-PdbViewer (http://www.expasy.org/spdbv/). Except for mutated residues, only secondary structures are visualized using ribbons. Panel A: whole complex V with indication of the main subunits; the c ring contains eight identical c subunits; dashed lines grossly indicate the limits of the inner mitochondrial membrane; extrinsic subunits protrude in the matrix; the blue rectangle borders subunit 6 (also called subunit a). Panel B: enlarged view of subunit a, showing the different mutated residues in white; Leu150Pro, Leu156Pro, Leu156Arg, Thr161Ser and Leu220Pro correspond to genomic mutations m8975T>C, m8993T>C, m8993T>G, m9008T>C and m9185T>C, respectively; note that in the bovine enzyme the human Leu150 is replaced by a phenylalanine. Panel C: subunit a with subunit b (green), and the closest two subunits c, labelled c7 (in yellow) and c8 (red), showing the interaction between Leu156 (white) of subunit a and Glu58 (red) of subunit c7. Panel D: view of the same subunits from the matrix side of the membrane better revealing Leu156 interaction with Glu58 and showing that other mutated residues do not interact with c subunits. Panel E: image obtained using the 3D-model of porcine mitochondrial ATP synthase (*pdb entry 6j5i*); secondary structures are visualized only for subunit a (blue) and subunit 8 (red). c subunits are coloured as in Panel C; subunit 8 mutated residue (Leu20) is in white; mutation Leu20Pro corresponds to genomic mutations m8424T>C; the two residues less than 4 Å distant from Leu20 by are indicated; both belong to subunit a; subunits that do not interact with subunit 8 Leu20 residue have been omitted.

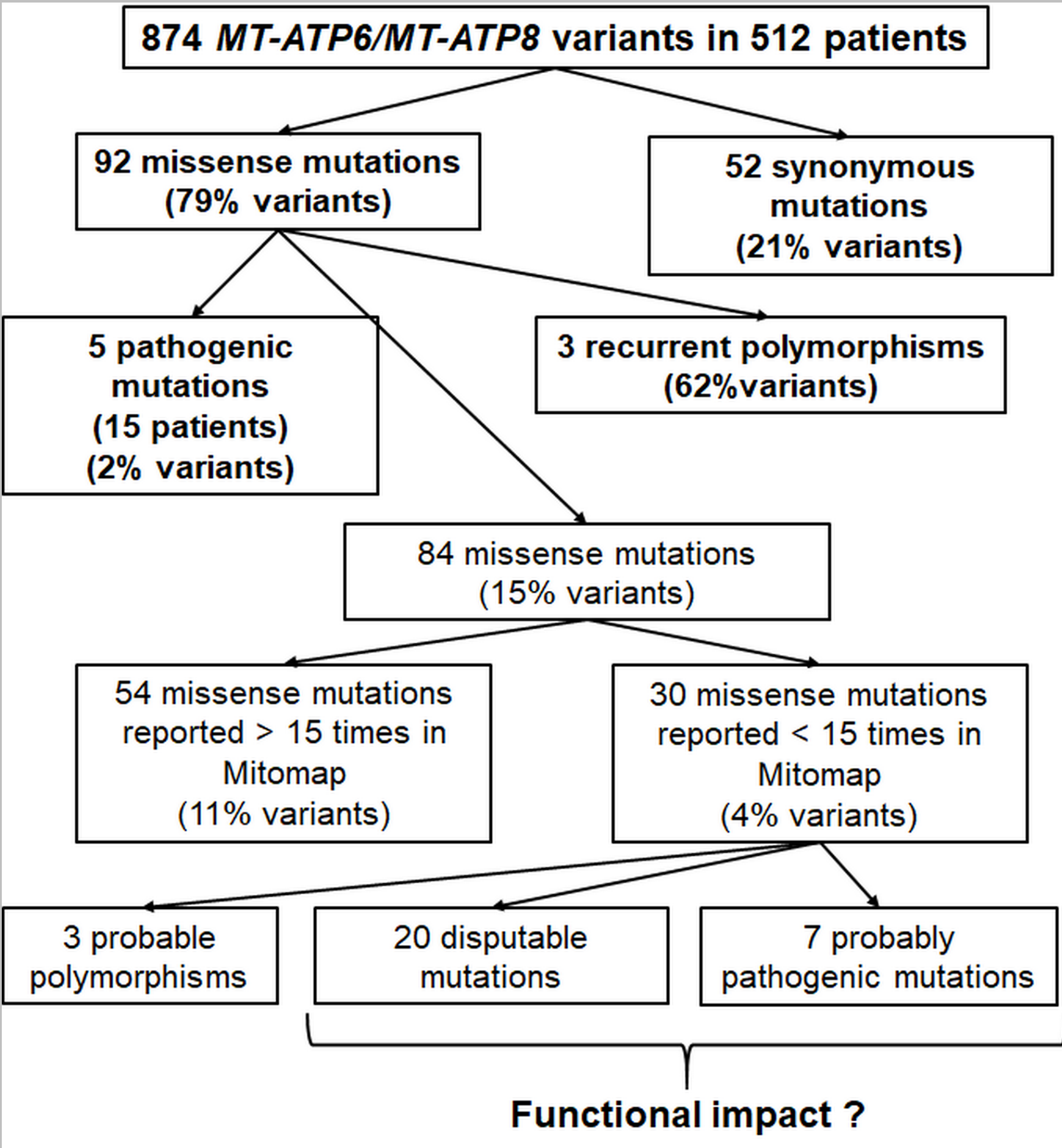
874 MT-ATP6/MT-ATP8 variants in 512 patients
92 missense mutations (79% variants)
52 synonymous mutations (21% variants)
5 pathogenic mutations (15 patients) (2% variants)
3 recurrent polymorphisms (62%variants)
84 missense mutations (15% variants)
54 missense mutations reported > 15 times in Mitomap (11% variants)
30 missense mutations reported < 15 times in Mitomap (4% variants)
3 probable polymorphisms
20 disputable mutations
7 probably pathogenic mutations
Functional impact ?

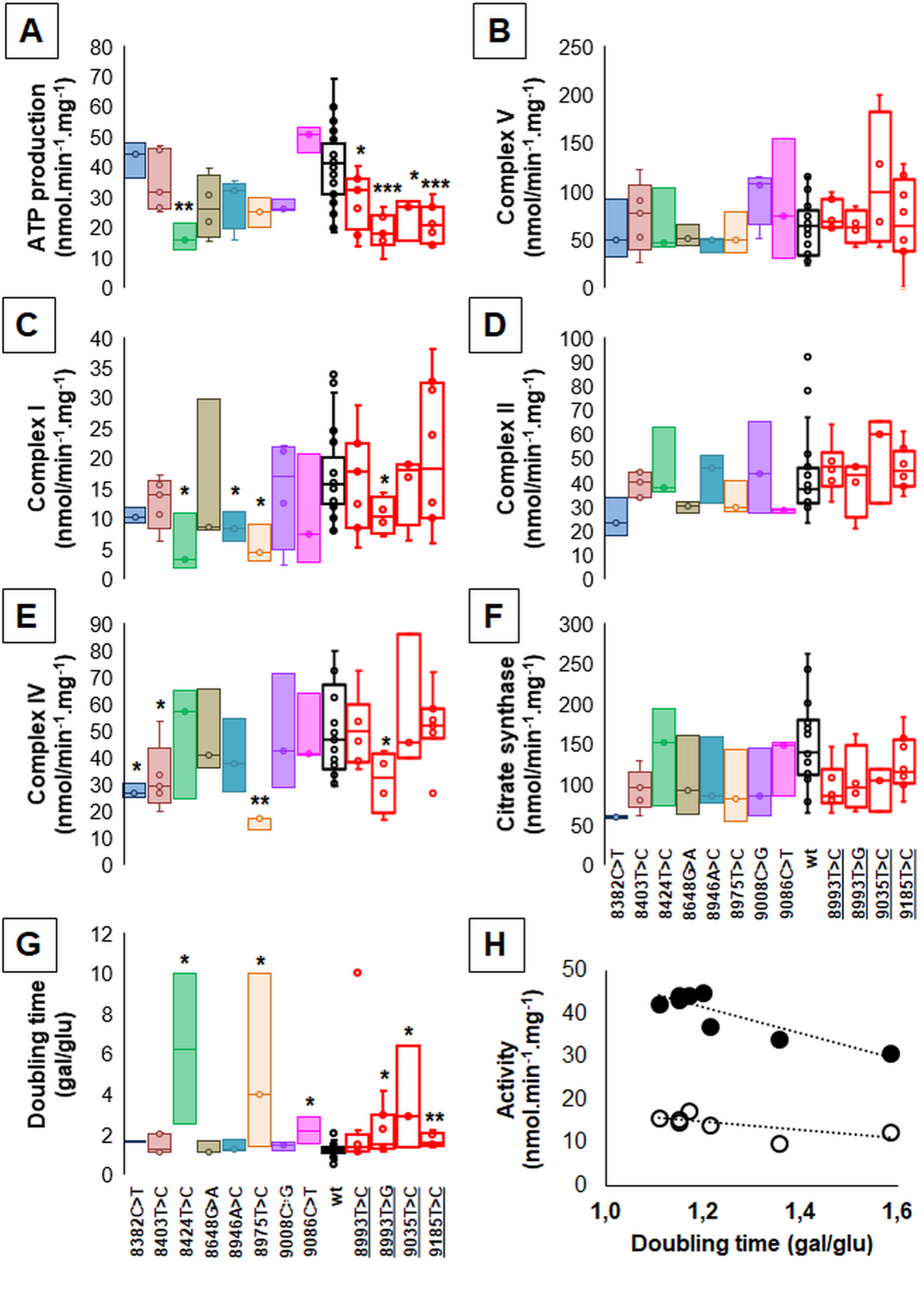
A
ATP production (nmol.min-1.mg-1)
B
Complex V (nmol/min-1.mg-1)
C
Complex I (nmol/min-1.mg-1)
D
Complex II (nmol/min-1.mg-1)
E
Complex IV (nmol/min-1.mg-1)
F
Citrate synthase (nmol/min-1.mg-1)
G
Doubling time (gal/glu)
H
Activity (nmol.min-1.mg-1)
Doubling time (gal/glu)
8382C>T
8403T>C
8424T>C
8648G>A
8946A>C
8975T>C
9008C>G
9086C>T
wt
8993T>C
8993T>G
9035T>C
9185T>C

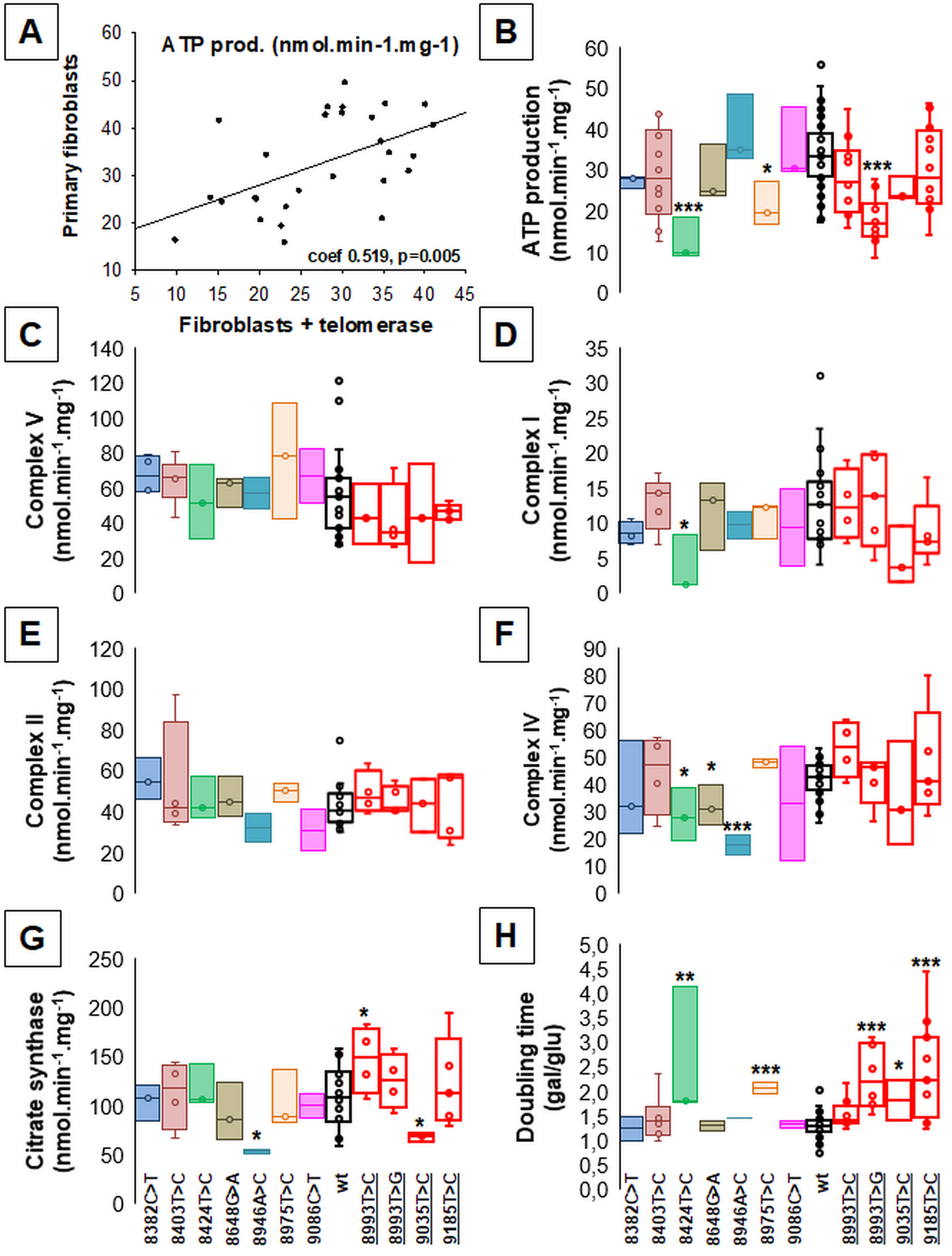
A
ATP prod. (nmol.min-1.mg-1)
Primary fibroblasts
coef 0.519, p=0.005
Fibroblasts + telomerase
B
ATP production (nmol.min-1.mg-1)
C
Complex V (nmol.min-1.mg-1)
D
Complex I (nmol.min-1.mg-1)
E
Complex II (nmol.min-1.mg-1)
F
Complex IV (nmol.min-1.mg-1)
G
Citrate synthase (nmol.min-1.mg-1)
H
Doubling time (gal/glu)
8382C>T
8403T>C
8424T>C
8648G>A
8946A>C
8975T>C
9086C>T
wt
8993T>C
8993T>G
9035T>C
9185T>C

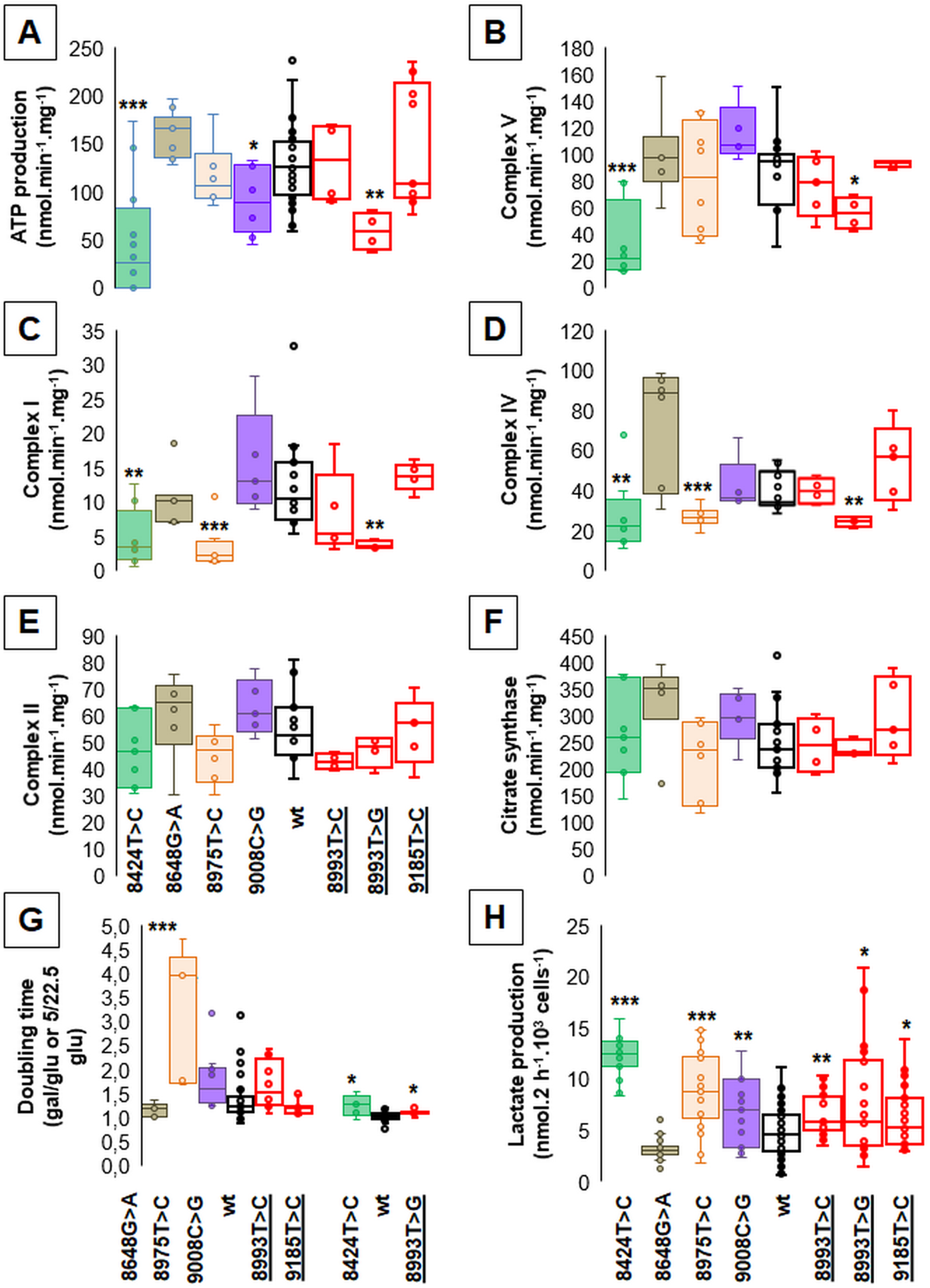
A
ATP production (nmol.min-1.mg-1)
B
Complex V (nmol.min-1.mg-1)
C
Complex I (nmol.min-1.mg-1)
D
Complex IV (nmol.min-1.mg-1)
E
Complex II (nmol.min-1.mg-1)
F
Citrate synthase (nmol.min-1.mg-1)
G
Doubling time (gal/glu or 5/22.5 glu)
H
Lactate production (nmol.2 h-1.10³ cells-1)
8424T>C
8648G>A
8975T>C
9008C>G
wt
8993T>C
8993T>G
9185T>C

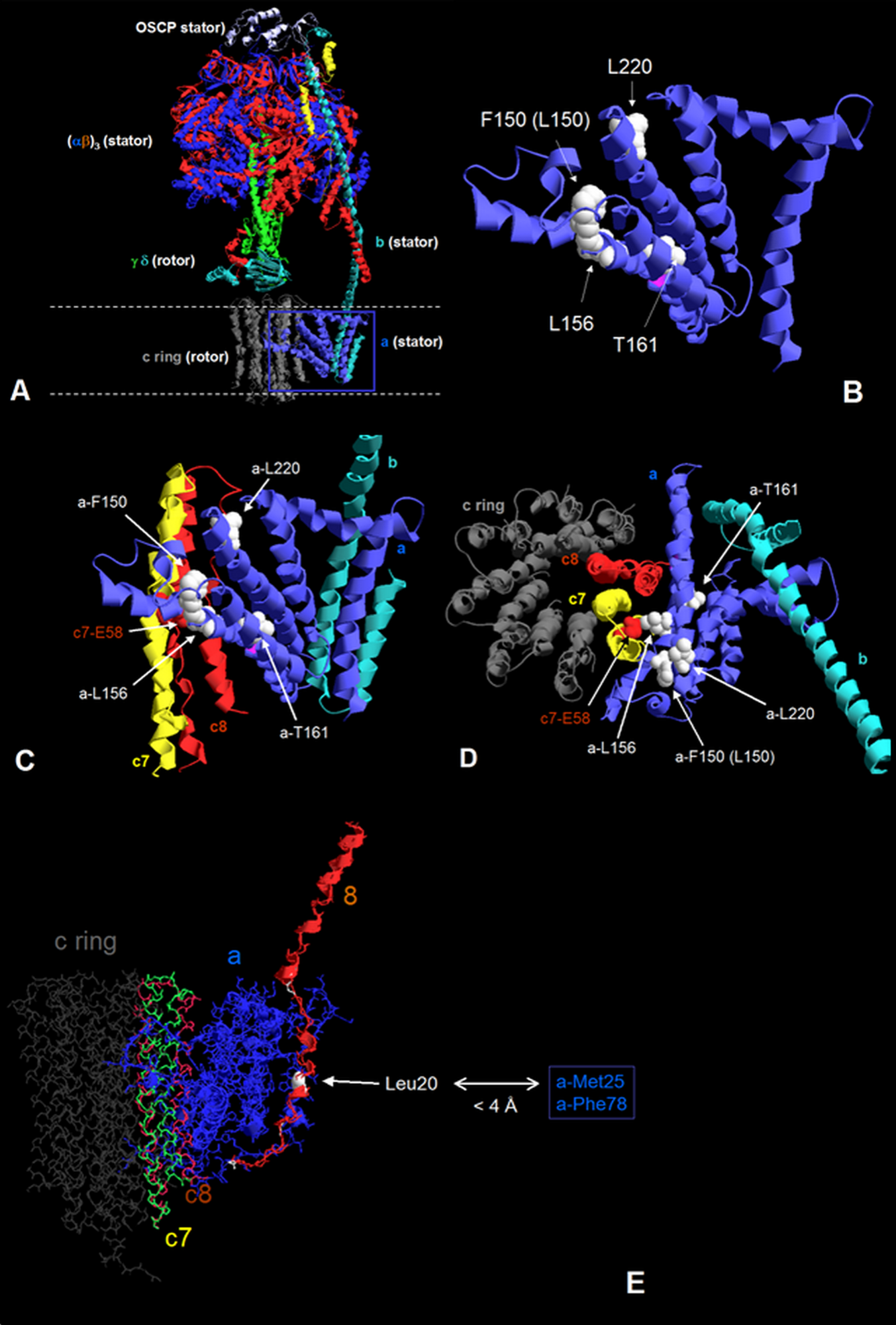
OSCP stator)
$(\alpha\beta)_3$ (stator)
b (stator)
γ δ (rotor)
c ring (rotor)
a (stator)
A
L220
F150 (L150)
L156
T161
B
a-L220
b
a-F150
a
c7-E58
a-L156
c8
a-T161
c7
C
c ring
a
a-T161
c8
c7
b
c7-E58
a-L220
a-L156
a-F150 (L150)
D
8
c ring
a
Leu20
< 4 Å
a-Met25
a-Phe78
c8
c7
E

Patient	http	Clinical presentation	Age	Lactate	Histology
8893T>C-1	100% (b+m)	PN, MD, CS, D	<5 (PN)/28/36	2.7	Denervation
8893T>C-2[1]	100% (b+u)	PN, EP	20 (EP)/34/42	N	Normal
8893T>C-3	100% (m)	E, D, MD, CS, PN	30(E)/61/62[†]	NA	Normal
8893T>G-1	100% (m+f)	LS	0.2(LS)/0.5/0.7[†]	3.9/4.6	NA
8893T>G-2	~100% (b)	E, MD, RP, PN	0.5 (E, MD)/0.5/18	NA	NA
8893T>G-3	~100% (m)	LS	0.2(LS)/1.7/1.7[†]	2.5/4.2	NA
9035T>C-1	100% (m+f)	MD/CS/PS/EP/PN	<10(MD)/31/34	2.2/2.2	NA
9176T>C-1[2]	100% (b)	EP/PN	16(EP)/36/44	NA	NA
9185T>C-2[3]	100% (b+u)	EP/PN	11(EP)/37/45	NA	NA
9185T>C-2[4]	100%(b)	EP/PN	11(EP)/31/39	NA	NA
9185T>C-3	100% (m)	PN, PS	47(PN)/51/61	NA	Normal
9185T>C-4	100% (b)	PN, MD	13(PN, MD)/15/20	High	NA
9185T>C-5	100% (b)	EP, PN	10(EP)/25/26	NA	NA
9185T>C-6	100% (b)	PN, PS	10(PN)/35/36	NA	NA
9185T>C-7	90%(b)	EP/PN	18(PN)/30/36	NA	NA

Table 1: Patients in the cohort presenting with confirmed *MT-ATP6/8* mutations

Patient are indicated by their mutation; [1]patient previously reported as Patient 8 in [22]; [2]= previously reported as Patient 7 in [22]; [3]=previously reported as Patient 4 in [22]; [4]=previously reported as Patient 5 in [22]. Http = heteroplasmy verification performed in the DNA extracted from the samples indicated between brackets; m = muscle biopsy, f = fibroblasts pellets; b = blood; u = urinary sediment. Clinical presentation: CS= Cerebellar Syndrome, D=deafness, E=Epilepsy, EP=Episodic paralysis; LS=Leigh Syndrome; MD=Mental Deficit; PN=axonal sensory-motor Peripheral Neuropathy; PS=Pyramidal Syndrome. Age is expressed as years; age at onset/age at

diagnosis/present age or age at death when marked by †. Histology = histological appearance of muscle. NA = data not available

Mutation	Residual muscle fragment			Initial muscle fragment				
Activity	CV		CI	CI	CII	CIII	CIV	CS
Inhibitor	IF1+oligo	oligo	rotenone	rotenone		antimycin		
m.8382C>T (6)	**78±8** (31±2%)	**63±3** (24±0%)	**17±1** (90±1%)					
m.8424T>C (6)	**40±15** (13±4%)	**6±5** (2±1%)	**25±2** (82±5%)	**9** (75%)	**15**	**112** (61%)	**85**	**120**
m.8806C>G (3)	166±7 (57±2%)	158±1 (54±5%)	ND	**21** (88%)	**39**	**108** (57%)	**96**	248
m.8902G>A (2)	170±20 (69±3%)	125±30 (52±7%)	28±3 (62±1%)					
m.8969G>C (6)	365±17 (87±1%)	329±9 (79±1%)	ND	**23** (68%)	72	155 (62%)	203	**336**
m.8975T>C (4)	**74±7** (51±3%)	**56±4** (39±1%)	**18±0** (84±6%)	41 (98%)	64	178 (70%)	239	223
m.9008C>G (4)	248±22 (55±2%)	216±19 (51±2%)	**26±0** (69±2%)					
m.9019A>G (4)	**129±16** (33±3%)	**94±13** (24±0%)	**8±1** (56±5%)	**4** (40%)	**16**	**83** (50%)	**65**	**78**
m.9035T>C	**46±5** (13±1%)	**19±26** (5±7%)	**15±1** (50±9%)	**23** (85%)	50	198 (79%)	224	181
m.9176T>C	**122±20** (28±4%)	**55** (13%)	89±5 (67±2%)					
Controls	266±95 [139] (73±14%)	228±90 [121] (65±11%)	42±14 [28] (89±10%)	42±14 [28] (89±10%)	62±19 [41]	160±59 [115] (67±7%)	199±57 [136]	209±64 [146]

Table 2: Spectrophotometric analysis of muscle fragments.

Underlined font indicate confirmed pathogenic mutations analyzed as pathologic controls. Numbers between brackets after the mutation recall the pathogenic score given by prediction software (6 being the highest score). Activities written in bold numbers are below the 10^{th} centile of control values. CV=complex V activity; IF1+oligo = complex V activity sensitive to oligomycin and IF1 added together; oligo = complex V activity sensitive to oligomycin alone; CI = complex I activity, which is the rotenone sensitive activity; numbers between brackets after activities values indicate the proportion of the specific complex activity in the total activity.

Residual muscle fragments = samples retrieved after identification of the mutation; initial muscle fragments = samples taken during the initial diagnostic investigations. For residual muscle fragments, values from patients are the mean and standard of assays performed on the same sample preparation. Number of assays = 4 for IF1+oligomycin sensitive complex V activity, 2 for oligomycin sensitive complex V activity and for rotenone sensitive complex I activity. Control values of complex V activity are the mean and standard deviation of the mean values obtained in 6 independent control samples, each assayed four or two times [24]. For initial muscle fragments and for complex I assay in residual muscle fragments, control values are the mean and standard deviation of the values obtained in 145 different control samples, each assayed once. ND = not done. Initial muscle fragments with mutation m.8424T>C or m.9019A>G disclosed low values for each measured activity, including complex II and citrate synthase. The high rotenone and antimycin sensitivity were against bad preservation of the sample, thus leaving the nature of the sample (fibrous for example) to incriminate.